BIOCHEMISTRY
including biophysical chemistry & molecular biology

Article

pubs.acs.org/biochemistry

Pseudomonas syringae Self-Protection from Tabtoxinine-β-Lactam by Ligase TblF and Acetylase Ttr

Timothy A. Wencewicz and Christopher T. Walsh*

Department of Biological Chemistry and Molecular Pharmacology, Harvard Medical School, 240 Longwood Avenue, Boston, Massachusetts 02115, United States

Supporting Information

ABSTRACT: Plant pathogenic *Pseudomonas syringae* produce the hydroxy-β-lactam antimetabolite tabtoxinine-β-lactam (TβL) as a time-dependent inactivating glutamine analogue of plant glutamine synthetases. The producing pseudomonads use multiple modes of self-protection, two of which are characterized in this study. The first is the dipeptide ligase TblF which converts tabtoxinine-β-lactam to the TβL-Thr dipeptide known as tabtoxin. The dipeptide is not recognized by glutamine synthetase. This represents a Trojan Horse strategy: the dipeptide is secreted, taken up by dipeptide permeases in neighboring cells, and TβL is released by peptidase action. The second self-protection mode is elaboration by the acetyltransferase Ttr, which acetylates the α-amino group of the proximal inactivator TβL, but not the tabtoxin dipeptide.

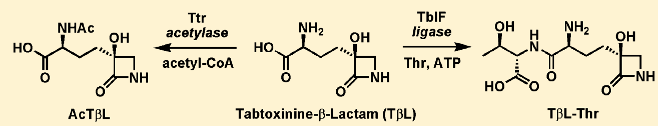

Pseudomonas syringae strains are found in epiphytic niches and have the capacity to be plant pathogens and invade plant tissues.[1,2] They can elaborate amino acid and peptide-based toxins that cause destruction of leaf tissue, necrosis, chlorosis, and release of nutrients. *P. syringae* specialize in the biosynthesis of nonproteinogenic amino acids that act as the phytotoxic antimetabolites.[3−5] Such toxins include coronatine, a hybrid polyketide-nonribosomal peptide that mimics jasmonate plant hormones in stomatal opening,[6−8] syringolin A with an electrophilic macrolactam that targets the plant proteasome,[9,10] phaseolotoxin, a tripeptide Trojan Horse precursor that releases the amino acid diaminophosphinyl-sulfamoyl ornithine, a picomolar inhibitor of ornithine transcarbamoylase,[11,12] and the nonribosomal peptides syringomycin and syringopeptins[13,14] that are membrane pore-formers.

Strains that are pathovars of tobacco, including *P. syringae* pvs *tabaci, coronofaciens, and garcae*[4] make and secrete a dipeptide tabtoxin (TβL-Thr or TβL-Ser), also known as wild fire toxin (Figure 1).[15] Tabtoxin contains the unusual amino acid tabtoxinine-β-lactam (TβL) and L-threonine (or, in a minor variant L-serine) and is an inactive precursor to the free TβL metabolite.[16,17] The Trojan Horse tabtoxin could liberate free TβL amino acid either during secretion through the periplasm or when taken up by the plant cells, via peptidase action.[18−20] TβL is misrecognized as glutamine by the plant glutamine synthetase and causes ATP- and time-dependent irreversible inactivation.[21−24] The exact mechanism of inactivation is not clear although a phosphorylated form of TβL has been proposed as a tight binding inhibitor.[16] Inhibition of Gln synthetase leads to a rise in intracellular NH_3 levels that is a proximal cause of the chlorosis characteristic of this infection.[25]

Tabtoxinine-β-lactam has a remarkable structure (Figure 1). As the name implies there is a four membered lactam that appears to have been fashioned on a lysine skeleton, utilizing C5 and C6 of the side chain. C5 also bears a hydroxyl group whose biosynthetic timing and origin is unclear. In addition, the carbonyl carbon of the β-lactam derives from an uncharacterized molecule of the C1 metabolic pool, so many puzzles remain about how this densely functionalized warhead is assembled since its structural characterization was completed in 1971.[16,26−28]

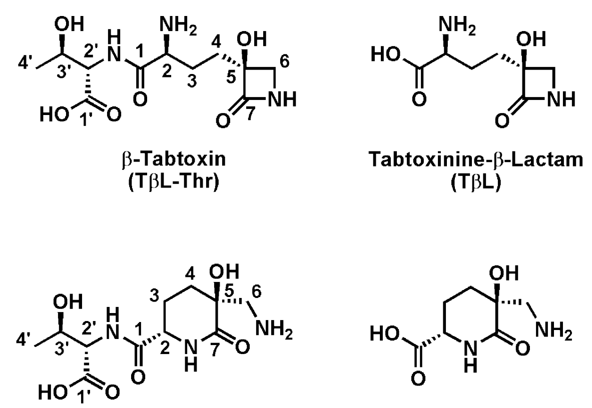

Figure 1. Structures of β-tabtoxin (TβL-Thr), tabtoxinine-β-lactam (TβL), δ-tabtoxin (TδL-Thr), and tabtoxinine-δ-lactam (TδL).

Transposon mutagenesis in a *P. syringae* producer strain led to identification of a cluster of biosynthetic genes,[29−31] some of which (*tabABD*) have homology to lysine biosynthetic genes.[32−34] Subsequent feeding studies indicated the TβL pathway diverges from the canonical Lys biosynthetic pathway at the level of tetrahydropicolinate.[26−28,34] The *tblSCDEF* genes

Received: August 22, 2012
Published: September 19, 2012

encode proteins that participate in the later stages of tabtoxin assembly.[31] Two additional enzymes have also been implicated. One is a metallopeptidase[31] presumed to be encoded by *tabP* that cleaves the tabtoxin dipeptide to tabtoxinine-β-lactam. It is proposed to be periplasmic and thus on pathway to generation of the active form of the toxin. A second, unlinked gene, *ttr*,[35] confers resistance when expressed in transgenic tobacco plants.[36] Structural studies with bound acetyl CoA indicate that Ttr should be an acetyl transferase, but its cosubstrate (e.g., tabtoxin vs tabtoxinine-β-lactam) has not been identified.[37−40] TblS and TblC are homologues of β-lactam synthase[41] and clavaminate synthase,[42] respectively, giving some hints about how lactam formation and hydroxylation may occur. TblF is homologous to dipeptide ligases with an ATP-grasp domain and may assemble tabtoxin from threonine and TβL or a precursor; it is not known whether the lactam and hydroxyl group are installed at the free amino acid or the dipeptide level.

Complicating study of this biosynthetic system is the scarcity of pure tabtoxin and tabtoxinine-β-lactam due to chemical lability built into both dipeptide and amino acid scaffolds, in the form of the amino group of the TβL moiety. Because tabtoxin is the dipeptide TβL-Thr and not Thr-TβL, the amine in both the tabtoxin dipeptide and in free TβL is available for favorable translactamization via intramolecular capture of the strained four membered lactam. Facile rearrangement in both acid and base yields the six membered δ-lactam in the dipeptide (isotabtoxin; TδL-Thr or TδL-Ser) and in free tabtoxinine (isotabtoxinine; TδL) (Figure 1). This rearranged δ-lactam is completely inactive biologically.[16] Preliminary reports on the half-lives of tabtoxin and tabtoxinine-β-lactam range from 24 h at neutral pH, 20 °C[16,43] to 15 min at pH 4.5, 20 °C,[43] but no rate data have been described.

Although syntheses of tabtoxin and TβL have been reported,[43−49] they are lengthy and we have chosen instead in this study to undertake isolation of the tabtoxin dipeptide from cultures of *P. syringae* pv *tabaci* ATCC 11528. Then we have utilized the Zn-dependent dipeptidase in producer crude lysates[19] to liberate free tabtoxinine-β-lactam. This approach gives pure samples of tabtoxin dipeptide and tabtoxinine-β-lactam amino acid for use in rearrangement rate studies to set a baseline for use of the labile β-lactam scaffolds in subsequent enzymatic studies. We report here on studies of two enzymes that protect the producer *P. syringae* from harm by the tabtoxinine-β-lactam. One is TblF, confirming it has dipeptide ligase activity and that TβL is a good substrate. The second is the Ttr enzyme which we show acetylates TβL but not the dipeptide tabtoxin or the δ-lactam forms.

■ MATERIALS AND METHODS

Strains, Materials, and Instrumentation. *P. syringae* pv *tabaci* ATCC 11528 was purchased from ATCC under USDA permit No. P526P-11-03463. DNA primers were purchased from Integrated DNA Technologies. Herculase II DNA polymerase was purchased from Agilent. Restriction enzymes and T4 DNA ligase were purchased from New England Biolabs. TOP10 *Escherichia coli* competent cells were purchased from Invitrogen. BL21-Gold(DE3) *E. coli* competent cells were purchased from Agilent. DH10B *E. coli* cells containing pJ201 vectors were purchased from DNA 2.0. Vector (pET-28a) was purchased from Novagen. PCR was performed on a Bio-Rad MyCycler thermal cycler. DNA purification was performed with kits purchased from Qiagen. DNA sequencing was performed by Genewiz. Nickel-nitrilotriacetic acid (Ni-NTA) agarose was purchased from Invitrogen. Any *k*D SDS-PAGE gels were purchased from Bio-Rad. Protein was dialyzed using 10,000 MWCO SnakeSkin Pleated Dialysis tubing from Thermo Scientific. Protein was concentrated using Amicon Ultra 10,000 MWCO centrifugal filters from Millipore. Restriction-grade thrombin was purchased from EMD Biosciences. Protein digests and MALDI analyses of peptide fragments were performed by the Dana-Farber Cancer Institute Molecular Biology Core Facility and peptide mass fingerprinting was performed using Mascot software. NMR solvents (D_2O and $(CD_3)_2SO$) were purchased from Cambridge Isotope Laboratories.

A pyruvate kinase/lactate dehydrogenase (PK/LDH) enzyme mix from rabbit muscle was purchased from Sigma-Aldrich as a buffered aqueous glycerol solution. All buffers, media, solvents, and reagents were purchased from Sigma-Aldrich unless otherwise noted. Amino acids and Fmoc-derivatized standards were purchased from Sigma-Aldrich, Bachem, or Novabiochem. N_6-Formyl-Lys-Thr, N_6-formyl-Lys-Ser, and their Fmoc-derivatives were synthesized as described in the Supporting Information (Scheme S1).

^{1}H and 2D NMR spectra were recorded on a Varian VNMRS 600 MHz spectrometer equipped with a triple-resonance probe and ^{13}C NMR spectra were recorded on a Varian MR 400 MHz spectrometer equipped with a OneNMR probe in 3 mm NMR tubes (Wilmad LabGlass). All ^{13}C NMR spectra taken in D_2O were referenced by spiking the sample with 0.05% v/v CH_3CN. NMR FIDs were processed with ACD/NMR Processor Academic Edition version 12.0 software. High resolution LC/MS data were collected on an Agilent Technologies 6520 Accurate-Mass Q-TOF LC/MS using a 50 × 2 mm Gemini 5 μ C18 100 Å column fit with a 4 × 2 mm guard cartridge (Phenomenex) or a 100 × 4.6 mm Luna 5 μ HILIC 200 Å column fit with a 4 × 3 mm guard cartridge (Phenomenex) and data were analyzed with MassHunter Qualitative Analysis version B.02.00 software. Analytical HPLC was carried out on Beckman Coulter System Gold instrument (126 solvent module, 168 detector, and 508 autosampler) using a 250 × 4.6 mm Luna 5 μ C18(2) 100 Å column fit with a 4 × 2 mm guard cartridge (Phenomenex) or a 250 × 4.6 mm 5 μm Supelco Discovery C18 column fit with a 4 × 2 mm guard cartridge (Sigma-Aldrich) and data were processed with 32 Karat version 7.0 software. Preparative HPLC was carried out on a Beckman Coulter System Gold instrument (126P solvent module and a 168 detector) using a 250 × 21.2 mm Luna 10 μ C18(2) 100 Å column fit with a 15 × 21.2 mm guard cartridge (Phenomenex) or a 150 × 21.2 mm Luna 5 μ HILIC 200 Å column fit with a 15 × 21.2 mm guard cartridge (Phenomenex) and data were processed with 32 Karat version 7.0 software. Protein purification was performed on an Amersham Pharmacia Biotech AKTA FPLC using a Sephadex 75 26/60 HiLoad prep grade gel filtration column (GE Healthcare). UV−vis spectrophotometry was performed on a Carey 50 Bio series spectrophotometer (Varian) with a PCB150 water peltier cooling system.

Cloning, Expression, and Purification of TabP, TblF, and Ttr. The TabP, TblF, and Ttr genes (*tabP* GenBank ID: AY083468, *tblF* GenBank ID: AY254169, and *ttr* GenBank ID: X17150) were optimized for expression in *E. coli*[50] and obtained as synthetic genes in pJ201 plasmids (DNA 2.0) encoded with *NdeI* and *Bam*HI restriction sites. The pJ201 plasmids were transformed into chemically competent TOP10 *E. coli* cells and amplified. The amplified plasmids were digested with NdeI and *Bam*HI-HF and the genes were gel purified. The genes were then ligated into vector pET-28a and transformed into chemically competent TOP10 *E. coli* cells. Proper gene insertion was confirmed by DNA sequencing of the purified plasmid DNA. The sequence-confirmed plasmid was then transformed into chemically competent BL21-Gold(DE3) *E. coli* cells for protein expression. For TabP-*N*-His_6, TblF-*N*-His_6, and Ttr-*N*-His_6 expressions the transformed cells were grown at 37 °C in 1 L batches of Luria broth (LB) media supplemented with 50 μg/mL kanamycin sulfate until an $OD_{600\ nm}$ of ~0.4 was reached. The temperature was then reduced to 15 °C and 0.5 mM IPTG was added to induce protein expression. The induced cultures were then incubated at 15 °C for 18 h with shaking (200 rpm) before cells were harvested by centrifugation (10000*g*, 25 min, 4 °C). Cells/protein were kept at 4 °C or on ice for all remaining purification steps. Cell pellets were resuspended in 40 mL of cold lysis buffer A (50 mM potassium phosphate pH 8.0, 500 mM NaCl, 5 mM β-mercaptoethanol, 20 mM imidazole, 10% glycerol), flash frozen, thawed, and then lysed by two passes through an Avestin EmulsiFlex-C5 homogenizer at 5000−15000 psi. Cell lysates were clarified by ultracentifugation (50000*g*, 35 min, 4 °C) and the supernatants were filtered through a 0.45 μm PES syringe filter before being treated with 7 mL of Ni-NTA resin pre-equilibrated in lysis buffer A using the batch method. Bound protein was eluted with lysis buffer B (50 mM potassium phosphate pH 8, 500 mM NaCl, 5 mM β-mercaptoethanol, 300 mM imidazole, 10% glycerol) and elution fractions were analyzed by SDS-PAGE with visualization by Coomassie blue staining. Protein identities were confirmed by mass finger-printing.

Proteins were then dialyzed into thrombin buffer (20 mM Tris pH 8.4, 150 mM NaCl, 1 mM $CaCl_2$, 1 mM dithiothreitol) for 4 h at 4 °C and concentrated to a final volume of 2−4 mL (TabP-*N*-His_6: 4 mL at 65 μM or 2.8 mg/mL; TblF-*N*-His_6: 3 mL at 360 μM or 17.3 mg/mL; Ttr-*N*-His_6: 2 mL at 512 μM or 11.0 mg/mL). Some precipitate formed during the dialysis of TabP-*N*-His_6 so the concentration of soluble protein produced during expression was determined from the Ni-NTA column elution fractions (20 mL of TabP-*N*-His_6 at 65 μM or 2.9 mg/mL). The *N*-terminal His_6-tags were removed by treatment with thrombin (0.02 unit thrombin/μmol protein) at 16 °C until complete cleavage was achieved as judged by SDS-PAGE analysis with Coomassie blue visualization (14−16 h). Proteins were further purified by gel filtration on a Sephadex 75 26/60 HiLoad column using an AKTA FPLC in S-75 buffer (50 mM potassium phosphate pH 8.0, 150 mM NaCl, 1 mM dithiothreitol, and 5% glycerol) at a flow rate of 2.0 mL/min at 4 °C. Fractions were analyzed by SDS-PAGE with Coomassie blue visualization (Supporting Information, Figures S1−S3) and those containing pure protein were pooled, concentrated, flash frozen, and stored at −80 °C. The final protein concentrations (TabP: 1.5 mL at 85.5 μM or 3.6 mg/mL; TblF: 2 mL at 410 μM or 19.7 mg/mL; Ttr: 3.0 mL at 276 μM or 5.4 mg/mL) were determined by UV−vis absorbance at 280 nm using the following exctinction coefficients calculated from the protein primary sequence using ExPASy Bioinformatics Research Portal: 40450 M^{-1} cm^{-1} for TabP, 77350 M^{-1} cm^{-1} for TblF, and 19940 M^{-1} cm^{-1} for Ttr.

Isolation and Purification of Tabtoxin. Six baffled Erlenmeyer flasks (3 L) containing 0.5 L of filter sterilized Woolley's[15] minimal media (10 g/L sucrose, 5 g/L KNO_3, 0.8 g/L K_2HPO_4, 0.8 g/L $NaH_2PO_4{\cdot}H_2O$, 0.2 g/L $MgSO_4{\cdot}7H_2O$, 0.1 g/L $CaCl_2{\cdot}2H_2O$, 20 mg/L $FeSO_4{\cdot}7H_2O$; Note: $FeSO_4{\cdot}7H_2O$ was added separately as a 1 mg/mL filter sterilized solution to prevent precipitation during media prep.) were inoculated with 0.5 mL of *P. syringae* ATCC 11528 preculture grown for 24 h in Difco Nutrient Broth (Becton, Dickinson and Company) to an OD_{600nm} of ~1. Inoculated flasks were shaken (225 rpm) at 26 °C in a Innova 44 incubator shaker (New Brunswick Scientific) for 66−73 h at which point the OD_{600nm} was ~1.5 and the pH had risen to ~7.4−7.8. Cells were removed by centrifugation (13500*g*, 60 min, 20 °C) and supernatants were diluted 1:1 with ethanol, the pH of each mixture was adjusted to ~4−5, and the mixtures were rested at 4 °C for 12 h to precipitate cell debris. The mixtures were centrifuged at 15250*g* for 60 min at 20 °C to remove cell debris and then slowly passed through preequilibrated (1:1 EtOH/H_2O) columns of Dowex 50WX8-200 cation exchange resin (4 × 2.5 cm for 1 L of ethanol-diluted supernatant). Columns were washed with H_2O and compounds were eluted with 100 mL of 4% aqueous NH_4OH and immediately flash frozen and lyophilized to give 150−200 mg of light tan solids that were determined by ^1H NMR and HRMS-ESI to be a mixture of TβL-Thr, TδL-Thr, TβL-Ser, and TδL-Ser. Treatment of a small aliquot of these crude solids with *P. syringae* cell lysates in the presence of Zn^{2+} ions, by the procedure described below, produced unrearranged TβL, the concentration of which could be determined using the TblF-PK-LDH coupled spectrophotometric assay, also described below. Assuming both TβL-Thr and TβL-Ser are cleaved by the *P. syringae* cell lysates, the amount of unrearranged tabtoxin dipeptides isolated from *P. syringae* cultures after elution from the Dowex column ranged from 7 to 11 mg/L of culture supernatant. (Determined using four independent cultures of *P. syringae* ATCC 11528 in 0.5 mL of Woolley's media.)

The crude solids were dissolved in 1:1 EtOH/H_2O (~10 mg/mL), filtered through a 0.2 μm filter, and purified by preparative HPLC using a 150 × 21.2 mm Luna 5 μ HILIC 200 Å column fit with a 15 × 21.2 mm guard cartridge with 5 mM ammonium formate in 90:10 CH_3CN:H_2O pH 3.2 (A) and 5 mM ammonium formate in 50:50 CH_3CN/H_2O pH 3.2 (B) as mobile phases (pH of mobile phases was adjusted with aq. HCl), a 1−2 mL injection volume, a flow rate of 12 mL/min, and detection at 210 nm. Samples were loaded in 20% B holding for 10 min and a linear gradient was then formed from 20% B to 60% B over 20 min. Fractions collected from 14 to 17 min contained primarily TβL-Thr with minor amounts of TδL-Thr and fractions collected from 17 to 19 min contained only TδL-Thr (Supporting Information; Figure S4).

Fractions containing TβL-Thr were further purified by prep-HPLC using a 250 × 21.2 mm Luna 10 μ C18(2) 100 Å column fit with a 15 × 21.2 mm guard cartridge using 0.1% TFA in H_2O (A) and 0.1% TFA in CH_3CN (B) as mobile phases, a 1 mL injection volume, a flow rate of 12 mL/min, and detection at 210 nm. Sample was loaded and eluted in 100% A with fractions collected from 7 to 9 min containing pure TβL-Thr (Supporting Information; Figure S5). Pure TβL-Thr was stored at pH 5.4 in ammonium formate buffer at −80 °C. ^1H, ^{13}C, and 2D NMR confirmed the structures and purity of TβL-Thr and TδL-Thr as described in the Supporting Information (Tables S3−S4; Figures S35−S40).

Hydrolytic Conversion of Tabtoxin to Tabtoxinine-β-Lactam with *P. syringae* Cell Lysate. A 0.5 L batch of *P. syringae* ATCC 11528 was grown in Woolley's media exactly as described above until 66−73 h or an OD_{600nm} of ~1.5 was reached. At this point a 50 μL aliquot of 100 mM $ZnCl_2$ (10 μM final concentration) was aseptically added and the flask was incubated for an additional 15 h. Cells were harvested by centrifugation (10000*g*, 45 min, 4 °C) and the supernatant was discarded. From this point forward *P. syringae* cells were kept at 4 °C or on ice. The cell pellet was washed twice with 30 mL portions of buffer (20 mM Tris pH 7.2, 250 mM NaCl, 50 μM $CaCl_2$, 10 μM $ZnCl_2$, 1 mM DTT, 5% glycerol) then resuspended in the same buffer and flash frozen. The freeze thawed cells were lysed by two passes through an Avestin EmulsiFlex-C5 homogenizer at 5000−15000 psi and clarified by centrifugation (17000*g*, 45 min, 4 °C). The supernatant was flash frozen and stored at −80 °C.

In a typical preparation of free TβL, purified TβL-Thr (3.9 mg, 7.9 mM final concentration) was dissolved in 1 mL of 0.1 M phosphate buffer at pH 6.5. *P. syringae* cell lysate supernatant (0.7 mL) was added and, if necessary, the pH was adjusted to 6.5 with 0.5 mM HCl or 0.5 mM NaOH. The mixture was gently rocked at 20 °C and periodically a 5 μL aliquot of the reaction mixture was quenched with 30 μL of 50 mM HCl and 50 μL of CH_3CN. The quenched aliquot was then Fmoc-labeled for HPLC visualization[51] by treatment with 50 μL of 0.2 M sodium borate pH 8.0 and 20 μL of 20 mM Fmoc-Cl in CH_3CN. After resting for 30 min, the quenched reaction aliquot was then treated with 20 μL of 0.1 M adamantylamine in CH_3CN, rested for 15 min, centrifuged (16000*g*, 15 min) to remove precipitate, and analyzed by analytical HPLC with detection at 263 nm using a 250 × 4.6 mm 5 μm Supelco Discovery C18 column fit with a 4 × 2 mm guard cartridge with mobile phases of 0.1% TFA in H_2O (A) and 0.1% TFA in CH_3CN (B). A gradient was formed from 20% B to 100% B over 25 min where Fmoc-TβL-Thr elutes at 12.9 min, Fmoc-TβL elutes at 13.6 min, and Fmoc-Thr elutes at 15.6 min. After 4 h nearly all of the TβL-Thr had been cleaved to TβL and Thr at which time the mixture was diluted with 1.7 mL EtOH, centrifuged (3500 rpm, 30 min, 4 °C), and filtered through a 0.2 μm syringe filter.

TβL was purified from this solution by prep-HPLC with detection at 210 nm using a 150 × 21.2 mm Luna 5 μ HILIC 200 Å column fit with a 15 × 21.2 mm guard cartridge with 5 mM ammonium formate in 90:10 CH_3N/H_2O pH 3.2 (A) and 5 mM ammonium formate in 50:50 CH_3CN/H_2O pH 3.2 (B) as mobile phases (pH of mobile phases was adjusted with aq. HCl), a 1 mL injection volume, a flow rate of 12 mL/min, and detection at 210 nm. Samples were loaded in 20% B holding for 10 min and a gradient was then formed from 20% B to 60% B over 20 min. Fractions collected from 9 to 11 min contained primarily Thr with minor amounts of TβL and fractions collected from 12 to 14 min contained pure TβL and only trace amounts of Thr (Supporting Information; Figure S6). TβL (1−5 mM) was stored at pH 5.4 in ammonium formate buffer at −80 °C. ^{1}H, ^{13}C, and 2D NMR confirmed the structure and purity of TβL and TδL as described in the Supporting Information (Tables S5−S6; Figures S41−S46).

Determination of β- to δ-Lactam Rearrangement Half-Lives for Tabtoxin Dipeptide and Tabtoxinine Amino Acid using ^{1}H NMR. Purified samples of TβL-Thr and TβL were dissolved in D_2O containing 50 mM potassium phosphate buffer at pH values of 5.4, 7.2, and 8.9. Samples also contained an unknown amount of residual ammonium formate and ammonium chloride salts from the prep-HPLC HILIC purification process. ^{1}H NMR were recorded at various time points and the diagnostic signals for TβL-Thr/TδL-Thr and TβL/TδL were integrated and first-order rate plots were generated as the natural log of relative percent TβL-Thr or TβL versus time to obtain the compound half-lives. See the Supporting Information for stack plots of ^{1}H NMR spectra, tables of peak integrations, and first-order rate plots (Figures S23−S34).

HPLC Assay for TblF Ligase Activity. For reactions using TβL as substrate: Reaction mixtures (100 μL) were incubated with gentle rocking at 20 °C and contained 1.1 μM TblF, 1.0 mM TβL, 1.0 mM amino acid coupling partner (L-Thr, L-Ser, L-homoSer, L-Ala, D-Thr), 10 mM $MgCl_2$, 5 mM ATP, and 50 mM HEPES (pH 7.5). Reaction progress was checked by quenching a 50 μL aliquot of the reaction mixture with 50 μL CH_3CN. The quenched mixture was then Fmoc-labeled for HPLC visualization[51] by treatment with 50 μL of 0.2 M sodium borate (pH 8.0) and 20 μL of 20 mM Fmoc-Cl in CH_3CN. After resting for 30 min, the mixture was treated with 20 μL of 20 mM adamantylamine in 1:1 CH_3CN/H_2O, centrifuged (12000*g*, 15 min), and analyzed by analytical HPLC with detection at 263 nm using a 250 × 4.6 mm 5 μm Supelco Discovery C18 column fit with a 4 × 2 mm guard cartridge with mobile phases of 0.1% TFA in H_2O (A) and 0.1% TFA in CH_3CN (B) where a gradient was formed from 20% B to 100% B over 25 min at a flow rate of 1 mL/min. Identity of the Fmoc-derivatized compounds were confirmed by high-resolution LC-MS using a 50 × 2 mm Gemini 5 μ C18 100 Å column fit with a 4 × 2 mm guard cartridge with mobile phases of 0.1% formic acid in H_2O (A) and 0.1% formic acid in CH_3CN (B) where sample (5 μL) was loaded in 5% B and held for 1 min then a linear gradient was formed from 5% B to 100% B over 15 min at a flow rate of 0.4 mL/min.

For reactions using N_6-formyl-L-lysine, N_6-acetyl-L-lysine, N_6-methyl-L-lysine, N_6-dimethyl-L-lysine, 5-DL−OH-DL-lysine, and L-lysine as substrates: Reaction mixtures (100 μL) were incubated with gentle rocking at 20 °C and contained 50 μM TblF, 2.5 mM N_6-formyl-L-lysine (or other lysine analogue), 2.5 mM amino acid coupling partner (L-Thr, L-Ser, L-homoSer, L-Ala, D-Thr, D-Ser), 10 mM $MgCl_2$, 5 mM ATP, and 50 mM HEPES (pH 7.5). Reaction progress was checked by quenching a 50 μL aliquot of the reaction mixture exactly as described above for TβL as a substrate. (See the Supporting Information, Table S1, for high-res LC-MS data.)

Determination of TβL Concentration Using a TblF-PK-LDH Coupled Spectrophotometric Assay. Reaction mixtures (250 μL) contained variable volumes (1.25−10 μL) of a TβL solution of unknown concentration, 20 mM L-Thr, 10 mM ATP, 12 mM $MgCl_2$, 0.5 mM PEP, 0.2 mM NADH, 100 mM HEPES (pH 7.5), 42 units/mL pyruvate kinase, 60 units/mL lactate dehydrogenase, and 2 μM TblF ligase. TblF was always added last to initiate the reaction. The reaction mixture was placed in a 1 cm quartz cell and monitored continuously at 350 nm for the oxidation of NADH to NAD^+ in a Carey UV−vis spectrophotometer at 20 °C until all TβL was consumed. The final absorbance was used to calculate the final concentration of NADH left at the end of the reaction using an extinction coefficient ε_{350} of 5650 M^{-1} cm^{-1} for NADH at 350 nm (determined experimentally by referencing to NADH concentration determined from the known ε_{340} of 6220 M^{-1} cm^{-1}).[52] The concentration of TβL was then determined from the linear slope of final micromoles NADH plotted versus volume of unknown TβL solution. All reactions were performed in duplicate. A representative set of graphed data is shown in the Supporting Information (Figures S14−S15).

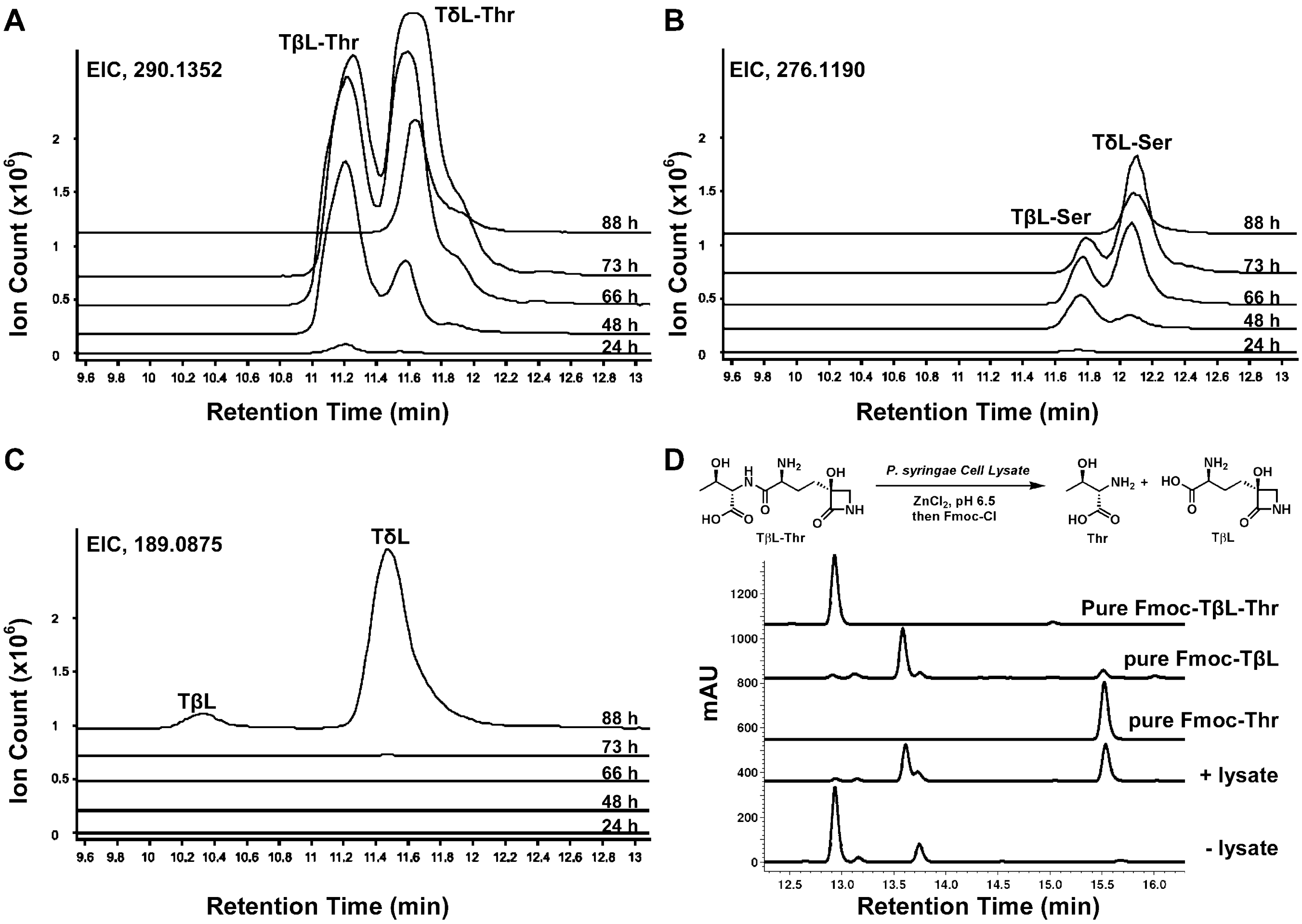

Figure 2. Isolation and purification of *β*-tabtoxin (T*β*L-Thr) and tabtoxinine-*β*-lactam (T*β*L) from cultures of *P. syringae* pv *tabaci* ATCC 11528 grown in Woolley's media.[15] Aliquots of culture supernatant (1 mL) were diluted with 1 mL of EtOH, filtered through a 0.2 *μ*m filter, and analyzed by high-resolution LC-MS (column: 100 × 4.6 mm Luna 5 *μ* HILIC 200 Å fit with a 4 × 2 mm guard cartridge; mobile phases: (A) 5 mM ammonium formate in 90:10 CH_3CN:H_2O, pH 3.2 and (B) 5 mM ammonium formate in 50:50 CH_3CN:H_2O, pH 3.2; gradient: load in 10% B and hold for 2 min then linear gradient formed from 10% B to 100% B over 15 min; injection volume: 8 *μ*L; flow rate: 0.5 mL/min) at various time points. Extracted ion chromatograms (EICs) were generated for (A) T*β*L-Thr/T*δ*L-Thr (EIC = 290.1352), (B) T*β*L-Ser/T*δ*L-Ser (EIC = 276.1190), and (C) T*β*L/T*δ*L (EIC = 189.0875). T*β*L-Thr was purified from *P. syringae* supernatant by stopping the culture after 66−73 h of growth, as described in the experimental section. Addition of $ZnCl_2$ (10 *μ*M) to the culture at the 73 h time point resulted in loss of T*β*L-Thr and T*β*L-Ser dipeptide peaks in the EIC chromatograms and appearance of T*β*L (minor) and T*δ*L (major) peaks at the 88 h time point. Since the desired *β*-isomer (T*β*L) was only present in minor amounts after treatment of *P. syringae* cultures with $ZnCl_2$ (C), a new approach was taken to obtain pure T*β*L. Purified T*β*L-Thr was treated with *P. syringae* cell lysates at pH 6.5 for 4 h in the presence of 10 *μ*M $ZnCl_2$ to quantitatively produce Thr and T*β*L which could subsequently be purified and used in enzymatic assays (D). Fmoc-derivatization was used only for visualization.[51] Underivatized T*β*L-Thr and T*β*L were both purified via prep-HPLC using a HILIC column as described in the Materials and Methods section. Retention times and observed masses from LC-MS analyses were as follows: T*β*L-Thr, calc. 290.1352, found 290.1347 at a retention time of 10.96 min; T*β*L-Ser, calc. 276.1190, found 276.1189 at a retention time of 11.57 min; T*δ*L-Thr, calc. 290.1352, found 290.1348 at a retention time of 11.36 min; T*δ*L-Ser, calc. 276.1190, found 276.1192 at a retention time of 11.83 min; T*β*L, calc. 189.0875, found 189.0867 at a retention time of 10.29 min; T*δ*L, calc. 189.0875, found 189.0868 at a retention time of 11.44 min.

Kinetics of TblF Ligase Activity Using a PK-LDH Coupled Spectrophotometric Assay for ADP Production. For all experiments, 250 *μ*L reaction mixtures contained 10 mM ATP, 12 mM $MgCl_2$, 0.5 mM PEP, 0.2 mM NADH, 100 mM HEPES (pH 7.5), 42 units/mL pyruvate kinase, and 60 units/mL lactate dehydrogenase. For determination of the T*β*L K_m value, reaction mixtures in addition contained 20 mM L-Thr, 50 nM TblF, and variable concentrations of T*β*L ranging from 0.53−17 *μ*M. For determination of the N_6-formyl-L-Lys K_m value, reaction mixtures in addition contained 20 mM L-Thr, 2 *μ*M TblF, and variable concentrations of N_6-formyl-L-Lys ranging from 0.5−32 mM. For determination of L-Thr and L-Ser K_m values, reaction mixtures in addition contained 17 *μ*M T*β*L, 50 nM TblF, and variable concentrations of L-Thr ranging from 0.16−40 mM or L-Ser ranging from 0.63−40 mM. For determination of the L-homoSer K_m value, reaction mixtures in addition contained 20 *μ*M T*β*L, 100 nM TblF, and variable concentrations of L-homoSer ranging from 1.25−40 mM. For determination of the L-Ala K_m value, reaction mixtures in addition contained 20 *μ*M T*β*L, 400 nM TblF, and variable concentrations of L-Ala ranging from 1.25−40 mM.

For all experiments, TblF ligase was added last to initiate the reaction. The reaction mixture was placed in a 1 cm quartz cell and monitored continuously at 350 nm in a Carey UV−vis spectrophotometer at 20 °C. Reaction velocities (k_{obs} in abs/min) were determined by calculating the slope of the initial

dx.doi.org/10.1021/bi3011384 | *Biochemistry* 2012, 51, 7712−7725

linear region of the 350 nm time course of each reaction. The change in NADH absorbance at 350 nm was converted to concentration using an ε_{350} of 5650 M^{-1} cm^{-1} for NADH (experimentally determined as described previously.[52] Kinetic constants were determined from velocity (k_{obs}) versus substrate concentration data using a nonlinear, least-squares fitting method with GraphPad Prism fit to the Michaelis–Menten equation (eq 1),

$$k_{obs} = \frac{k_{cat}[S]}{K_m + [S]} \tag{1}$$

where k_{cat} is the maximal velocity, [S] is the substrate concentration, and K_m is the susbrate concentration that yields $k_{obs} = 1/2k_{cat}$. All reactions were performed in triplicate.

Ttr HPLC Acetylase Activity Assay. For the acetylation of TβL, reaction mixtures (150 μL) were incubated with gentle rocking at 20 °C and contained 25 μM Ttr, 1.5 mM TβL, 1.5 mM AcCoA, and 25 mM HEPES (pH 7.5). Reaction progress was checked by quenching a 20 μL aliquot of the reaction mixture with 130 μL of 50 mM aqueous HCl. The quenched mixture was then analyzed by analytical HPLC with detection at 210 nm using a 250 × 4.6 mm Luna 5 μ C18(2) 100 Å column fit with a 4 × 2 mm guard cartridge with a mobile phase of 0.1% TFA in H_2O (A) where TβL elutes at 3.4 min and AcTβL elutes at 7.6 min.

For the acetylation of lysine analogs, reaction mixtures (100 μL) were incubated with gentle rocking at 20 °C and contained 25 μM Ttr, 1.5 mM lysine analogue (L-lysine, N_6-formyl-L-lysine, N_6-acetyl-L-lysine, or N_1-acetyl-L-lysine) 1.5 mM AcCoA, and 25 mM HEPES (pH 7.5). Reaction progress was checked by quenching a 20 μL aliquot of the reaction mixture with 130 μL of 50 mM aqueous HCl and analyzing the mixture by high-resolution LC-MS using a 50 × 2 mm Gemini 5 μ C18 100 Å column fit with a 4 × 2 mm guard cartridge with mobile phases of 0.1% formic acid in H_2O (A) and 0.1% formic acid in acetonitrile (B) where sample (12 μL) was loaded in 0% B and held for 5 min and a linear gradient was then formed from 0% B to 100% B over 10 min with a flow rate of 0.4 mL/min. (See the Supporting Information for LC/MS data; Figures S19–S22 and Table S2.)

Purification and Structure Elucidation of Ttr Product (AcTβL). TβL (0.86 mg, 0.0046 mmol) was acetylated with Ttr by the procedure described above. The reaction mixture was quenched by the addition of 1 volume equivalent of EtOH, centrifuged (16000*g*, 30 min, 4 °C), and filtered through a 0.2 μm syringe filter. AcTβL was purified from this solution by prep-HPLC using a 250 × 21.2 mm Luna 10 μ C18(2) 100 Å column fit with a 15 × 21.2 mm guard cartridge and 0.1% TFA in H_2O (A) as mobile phase, a 1 mL injection volume, a flow rate of 12 mL/min, and detection at 210 nm. Fractions collected from 15 to 17 min contained pure AcTβL (Supporting Information; Figure S7). The structure of AcTβL was elucidated by ^{1}H, ^{13}C, and 2D NMR as described in the Results and Discussion section and the Supporting Information (Table S7 and Figures S47–49).

RESULTS AND DISCUSSION

Isolation and Purification of Tabtoxin and Tabtoxinine-β-lactam. To obtain the dipeptide tabtoxin and the free amino acid tabtoxinine-β-lactam we evaluated production from the known toxin producer *P. syringae* pv *tabaci* ATCC11528 in Woolley's media[15] at 26 °C. Neither the dipeptide nor the free β-lactam amino acid have robust chromophores and are extremely polar which makes their separation and detection in culture supernatants difficult by standard methods. We utilized high-res LC-MS with a hydrophilic interaction chromatography (HILIC) column to separate and identify metabolites excreted into the culture supernatants over the course of growth. We could detect tabtoxin dipeptides, TβL-Thr and TβL-Ser, after 48 h of growth with a maximum yield at 66 h of growth. Increasing amounts of isotabtoxin dipeptides, TδL-Thr and TδL-Ser, continued to build throughout the entire growth phase while the amounts of TβL-Thr and TβL-Ser remained relatively constant from the 66 h time point to the end (Figure 2a,b). Addition of 10 μM $ZnCl_2$[26] at the 73 h time point followed by 15 h of continued growth resulted in quantitative cleavage of tabtoxin dipeptides (TβL-Thr and TβL-Ser; Figure 2a,b) and formation of tabtoxinine-β/δ-lactam isomers, TβL and TδL (Figure 2c).

Unfortunately, after the addition of Zn^{2+} tabtoxinine-δ-lactam (TδL) was the major metabolite present. Purification and isolation of the desired TβL isomer proved to be difficult. Therefore, we decided to isolate the more prominent tabtoxin dipeptide (TβL-Thr) by stopping culture growth after 73 h (OD_{600} ~1.5; pH ~7.4–7.8). To isolate TβL-Thr, 0.5 L of cells were removed by centrifugation and culture supernatant was diluted 1:1 with ethanol and pH adjusted w/6 N HCl to ~4–5 to precipitate cell debris. The diluted supernatant was passed through a strongly acidic Dowex 50WX8–200 cation exchange resin and compounds were eluted with 4% aqueous NH_4OH. After lyophilization the resulting solid was purified by preparative HPLC using a HILIC column to give pure TβL-Thr (~5–10 mg/L *P. syringae* culture). With pure tabtoxin dipeptide in hand we turned to an enzymatic route to release the unrearranged Tβl amino acid from TβL-Thr.

Hydrolytic Conversion of Tabtoxin to Tabtoxinine-β-Lactam without Rearrangement. Our first effort involved heterologous overproduction of TabP, a proposed zinc-dependent dipeptidase.[31] Although expression and purification of soluble enzyme from *E. coli* was obtained (58 mg/L; Supporting Information, Figure S1), we were unsuccessful in demonstrating dipeptidase activity on tabtoxin. Initial isolation studies and partial purification from *P. syringae* strains had noted the instability of this enzyme preparation.[19] Therefore, after multiple efforts to coax the anticipated activity we turned instead to follow the observation that when zinc ions are added to cultures of *P. syringae* producers, the secreted metabolite profile switches from largely tabtoxin dipeptide to free TβL (Figure 2a,b,c).[26] The presumption is that TabP is periplasmic and zinc limited, but in the presence of the cofactor divalent cation TabP can cleave tabtoxin on the way out of the producing cell.

We then grew *P. syringae* under producing conditions in the presence of 10 μM $ZnCl_2$ until an OD_{600} of ~1.5 was reached. Cells were collected, washed, and lysed in buffer containing 10 μM $ZnCl_2$. This cell lysate preparation was mixed with purified TβL-Thr at a final pH of ~6.5 and dipeptide cleavage was monitored by quenching the mixture with Fmoc-Cl and analyzing by HPLC with detection at 263 nm.[51] As shown in Figure 2d, the tabtoxin dipeptide is hydrolyzed to threonine and free tabtoxinine-β-lactam, presumably by TabP activated in those extracts. Tabtoxinine-β-lactam and Thr were then further purified in their underivatized form by preparative HPLC using a HILIC column and characterized by NMR and HRMS. Purification of tabtoxin from *P. syringae* cultures followed by

dx.doi.org/10.1021/bi3011384 | *Biochemistry* 2012, 51, 7712–7725

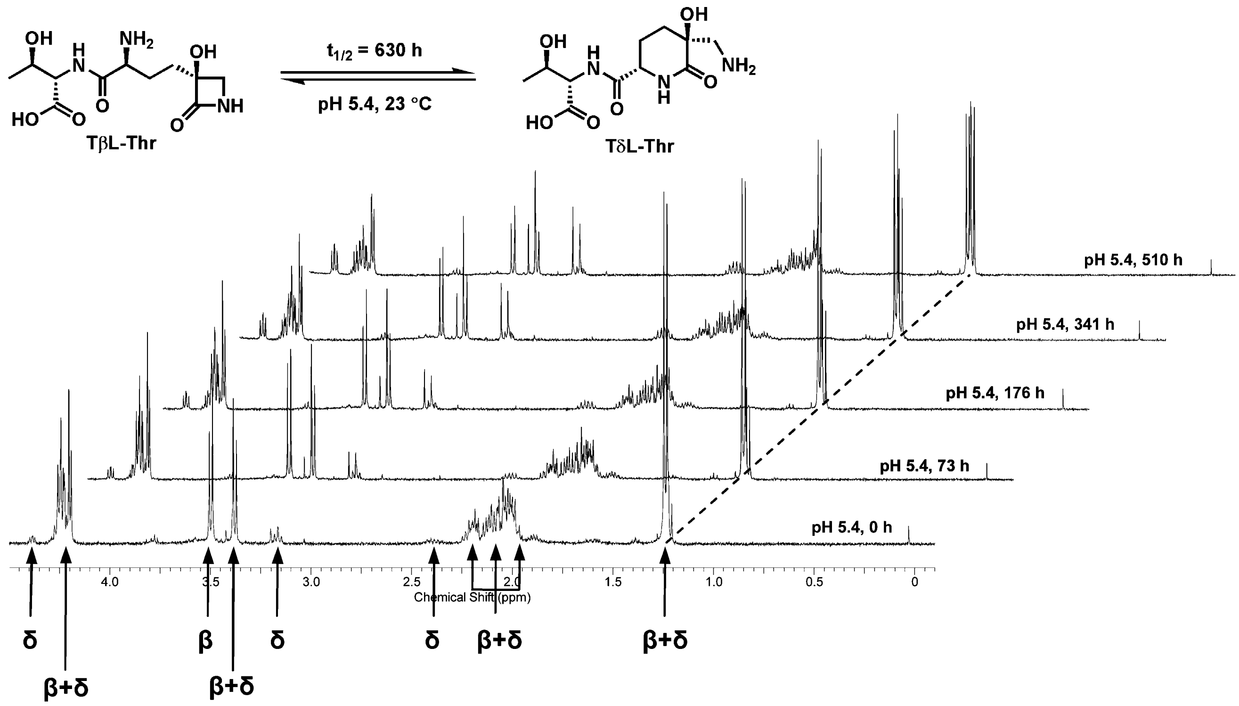

Figure 3. Rearrangement of TβL-Thr to TδL-Thr at pH 5.4 in D_2O at 23 °C containing 50 mM potassium phosphate buffer monitored by ^{1}H NMR. See the Supporting Information, Figures S23−S34, for more ^{1}H NMR stack plots and first order rate plots at pH values of 5.4, 7.2, and 8.9.

cell lysate cleavage of the dipeptide yields 7−11 mg TβL/L of culture, in turn allowing mg quantities of TβL to be generated and purified. The true amount of TβL produced by the cultures of *P. syringae* in Woolley's media was greater than 7−11 mg/L of culture, but the majority is lost due to the facile rearrangement of TβL-Thr and TβL-Ser to TδL-Thr and TδL-Ser, respectively. The amount of potential TβL lost to isotabtoxin dipeptides is difficult to quantify, but a conservative estimate based on HRMS analysis and purified TδL-Thr isolated is >30 mg TβL/L lost to the β/δ rearrangement.

Formation of the Inactive δ-Lactams from Tabtoxin Dipeptide and TβL Free Amino Acid by ^{1}H NMR Analyses. Next we turned to determination of the rearrangement rates of the β-lactam to the inactive δ-lactam in the framework of both the dipeptide tabtoxin and the free amino acid tabtoxinine-β-lactam to determine reasonable storage conditions and also for conditions to conduct enzyme assays described below. A straightforward approach to assess the inactivating rearrangement rates was to record ^{1}H NMR spectra at 23 °C in buffered D_2O under a range of pH values and monitor the diagnostic resonances as the β- to δ-lactam rearrangement proceeds (Figure 3). Both the dipeptide, TβL-Thr, and amino acid, TβL, were most stable at pH 5.4 with half-lives of 26 and 48 days, respectively. At pH 7.2 the β to δ rearrangement was significantly faster with half-lives of 37 h for TβL-Thr and 133 h for TβL and was still faster yet at pH 8.9 with half-lives of 15 h for TβL-Thr and 12 h for TβL (Table 1). Interestingly, TβL-Thr and TβL are both most stable (pH 5.4) within the reported pH optimum (4.0−5.5 pH units) for active transport into corn cells via dipeptide permeases.[20] On the basis of these data we chose to run enzymatic assays at pH 6.5−7.5 in nonnucleophilic buffers at 23 °C and we stored both tabtoxin and TβL at pH 5 in ammonium formate buffer at −80 °C.

Dipeptide Ligase Activity of TblF. Tabtoxin has been isolated as both the L-Thr (TβL-Thr) and L-Ser (TβL-Ser)

Table 1. Half-Lives of Isomerization for TβL-Thr/TδL-Thr and TβL/TδL at 23 °C and Various pH Values[a]

	half-life (h)		
compound	pH 5.4	pH 7.2	pH 8.9
TβL-Thr	630	37	15
TβL	1155	133	12

[a]First-order kinetic plots were generated by ^{1}H-NMR time course studies in 50 mM phosphate buffer in D_2O.

dipeptides with TβL-Thr being the major dipeptide in the mixture. Indeed in our hands both TβL-Thr and TβL-Ser were produced by *P. syringae* (Figure 2) with TβL-Thr being the major dipeptide observed. Presumably both tabtoxin dipeptides are assembled by the same dipeptide ligase, TblF. Bioinformatics analysis suggests that TblF is a dipeptide ligase with an ATP-grasp domain,[53] similar to the well characterized ligases BacD in bacilysin[54−56] and DdaF in dapdiamide [57] biosynthetic pathways. It was shown that ^{14}C-labeled L-Thr was incorporated into tabtoxin dipeptide by a nonribosomal pathway, but no assays with purified enzyme have been reported.[58] The free amino acid TβL is the known glutamine synthetase inactivator while the dipeptide tabtoxin is no longer recognized by the target enzyme, thus providing the producer organism some level of self-protection. The biological substrate and timing of dipeptide formation is still unknown. This knowledge would offer insights into the TβL biosynthetic route including whether lactam formation and hydroxylation occurs at the level of free amino acid or dipeptide. We were interested in evaluating the function of TblF as an amino acid ligase to validate its ability to couple both L-Thr and L-Ser as well as other C-terminal amino acids to TβL, verify its regioselectivity, and determine if the fully elaborated TβL scaffold, compared to a variety of lysine analogs, is the likely biological substrate presumed to be ligated as a dipeptide in a self-protective mode.

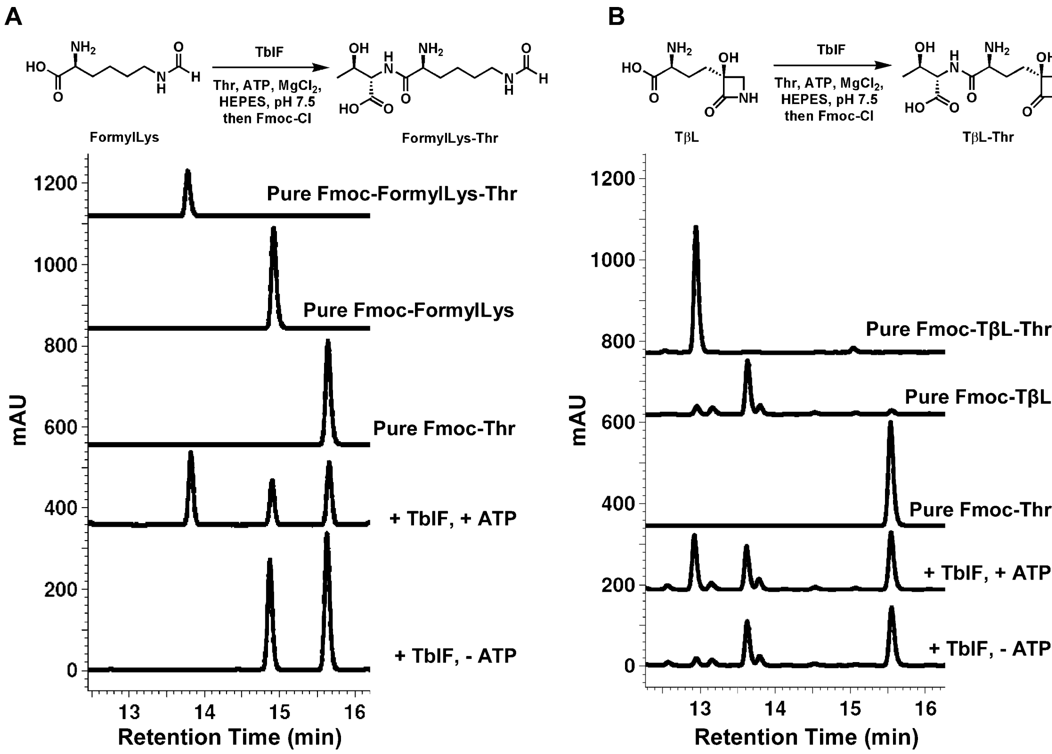

Figure 4. Characterization of TblF activity by HPLC analysis with detection at 263 nm showing ATP-dependent ligation of (A) a model substrate, N_6-formyl-L-lysine (FormylLys), and physiological substrate (B) TβL with L-Thr. Fmoc-derivatization was used only for visualization of the substrates and products.[51]

To that end recombinant TblF-*N*-His$_6$ fusion was overproduced in and purified from *E. coli* as a soluble enzyme (yield = 52 mg/L; Supporting Information, Figure S2). After cleavage of the *N*-His$_6$ tag with thrombin and purification by size exclusion chromatography, TblF at 50 μM was evaluated for ligase activity using a variety of lysine analogues (N_6-formyl-L-lysine, N_6-acetyl-L-lysine, N_6-methyl-L-lysine, N_6-dimethyl-L-lysine, 5-DL-OH-DL-lysine, and L-lysine) and L-Thr, both substrates at 2.5 mM, in the presence of excess ATP and $MgCl_2$. Since the amino acids and corresponding dipeptides have no chromophore they were converted to their Fmoc derivatives [51] for analysis by HPLC with detection at 263 nm as well as LC-MS analysis. All of the lysine analogs gave some detectable dipeptide with L-Thr and there was a clear trend in the relative amounts of product formed: N_6-formyl-L-lysine > L-lysine > N_6-acetyl-L-lysine > 5-DL-OH-DL-lysine > N_6-methyl-L-lysine > N_6-dimethyl-L-lysine. (Note: Relative amounts were judged by LC-MS using EIC ion counts and relative peak heights of the Fmoc-derivatized dipeptides. No effort was made to further quantify the amounts of dipeptide formed for these reactions. No homocoupled dipeptides could be detected by high resolution LC-MS. See the Supporting Information, Table S1 and Figures S8–S13, for HPLC traces and LC-MS data.)

The reaction between N_6-formyl-L-lysine and L-Thr is noteworthy because it gave significantly more dipeptide than the other lysine analogues (Figure 4a and Supporting Information, Figure S10a) and is most structurally similar to TβL since it has one extra carbon unit appended to the epsilon nitrogen. Synthesis of N_6-formyl-L-lysine-L-Thr dipeptide and its Fmoc-derivative (Supporting Information, Scheme S1) confirmed the regiochemistry of TblF as only N_6-formyl-L-lysine-L-Thr dipeptide isomer was formed.

With active TblF in hand we next evaluated its activity using TβL, generated from Zn^{2+}-peptidase-mediated hydrolysis of tabtoxin as noted in an earlier section, and L-Thr. The TblF reaction between TβL and L-Thr was rapid and went to completion, so less enzyme (1 μM) and substrates (1 mM) were ultimately used in the Fmoc-derivative HPLC assay (Figure 4b). The Fmoc-derivatized TblF product, Fmoc-TβL-Thr, had identical mobility to authentic Fmoc-TβL-Thr dipeptide isolated from *P. syringae*. The δ-lactam isomer, TδL, was not a substrate for TblF (Supporting Information, Figure S12d).

The HPLC assay indicated that TβL was a much better substrate than N_6-formyl-L-lysine so we sought to quantify this by carrying out kinetics on TblF. To achieve this we took advantage of the fact that TblF cleaves ATP to ADP and P_i during ligation, presumably generating the TβL aminoacyl phosphate as the activated intermediate which is then captured by the amino group of L-Thr. A coupled enzymatic spectrophotometric assay with pyruvate kinase (PK) and lactate dehydrogenase (LDH) was used to calculate kinetic parameters at 20 mM L-Thr by monitoring NADH conversion to NAD^+ at 350 nm, a reaction that is triggered by ADP formation in this coupled assay. As described in the Materials and Methods section, this TblF-PK-LDH coupled spectrophotometric assay was routinely used to determine the concentration of TβL which was critical for determining kinetic parameters and calibrating TβL solutions for use in enzymatic assays. For N_6-formyl-L-lysine, a K_m value of 2.8 mM and a k_{cat} value of 43.9 min^{-1} were recorded (Table 2). For TβL, a K_m value of 1.6 μM and a k_{cat} value of 68.6 min^{-1} were found, representing a k_{cat}/K_m catalytic efficiency ratio of ~2000 fold enhanced over N_6-formyl-L-lysine. While each of the lysine analogs, including N_6-formyl-L-lysine, screened in the TblF

Table 2. TblF Kinetics with Respect to Tabtoxinine-β-lactam (TβL) and N_6-Formyl-L-lysine (FormylLys) and at a Fixed L-Thr Concentration of 20 mM[a]

substrate	k_{cat} (min^{-1})	K_m (μM)	k_{cat}/K_m (μM^{-1} min^{-1})
TβL	68.6 ± 1.8	1.6 ± 0.1	42.9
formylLys	43.9 ± 0.8	2798 ± 866	0.02

[a]Kinetics were performed using a coupled enzymatic assay with pyruvate kinase (PK) and lactate dehydrogenase (LDH) monitoring for NADH consumption at 350 nm. Values are best fit ± standard error from three independent experiments.

HPLC assay represent potential advanced intermediates in the biosynthetic pathway, the kinetic data suggest that the fully elaborated TβL scaffold is the most relevant physiological substrate.

Kinetic parameters for L-Thr, L-Ser, L-homoSer, and L-Ala reacting with TβL were also determined using the TblF-PK-LDH coupled spectrophotometric assay (Table 3). The K_m for

Table 3. TblF Kinetics with Respect to L-Thr, L-Ser, L-homoSer, and L-Ala at a Fixed TβL Concentration of 20 μM[a]

substrate	k_{cat} (min^{-1})	K_m (mM)	k_{cat}/K_m (mM^{-1} min^{-1})
L-Thr	66.4 ± 1.5	2.6 ± 0.2	25.5
L-Ser	83.9 ± 2.2	10.3 ± 0.7	8.1
L-homoSer	56.2 ± 1.9	57.1 ± 3.0	1.0
L-Ala	31.7 ± 3.4	91.0 ± 12.9	0.3

[a]Kinetics were performed using a coupled enzymatic assay with pyruvate kinase (PK) and lactate dehydrogenase (LDH) monitoring for NADH consumption at 350 nm. Values are best fit ± standard error from three independent experiments.

Thr as cosubstrate for TβL was 2.6 mM and the k_{cat} was 66.4 min^{-1}. As mentioned earlier, a minor variant of tabtoxin produced by *P. syringae* has L-ser in place of L-Thr. Indeed, TblF utilized L-Ser as C-terminal substrate for condensation with TβL with a k_{cat} of 83.9 min^{-1} and K_m value for L-Ser of 10.3 mM for about a 3-fold decrease in catalytic efficiency (k_{cat}/K_m) compared to L-Thr. L-homoserine and L-alanine were used even less efficiently by TblF with K_m values of 57.1 and 91.0 mM, respectively, and k_{cat} values of 56.2 and 31.7 min^{-1}, respectively. These kinetic studies reveal that L-Thr is the preferred substrate for coupling with TβL and that the observation of minor amounts of L-Ser tabtoxin dipeptide (TβL-Ser) in *P. syringae* extracts is justified by the 3-fold decrease in TblF catalytic efficiency for L-Ser compared to L-Thr.

TblF clearly prefers tabtoxinine-β-lactam over N_6-formyl-Lys and other modified lysine analogs. The function of TblF is thus most probably a self-protection catalyst, sweeping nascent, active TβL in the producing cell into the tabtoxin dipeptide, inactive as a glutamine synthetase inactivator, which serves as a Trojan Horse reagent for export and subsequent uptake by plant cells. It is curious that the ligase makes the TβL-Thr dipeptide regioisomer rather than the Thr-TβL isomer. One would think that either regioisomer would have served the purpose of self-protection. However, in tabtoxin the amino group of the TβL residue is still free and can engage in intramolecular attack at the lactam carbonyl to yield the biologically dead δ-lactam version of the dipeptide, not resuscitatable as an antimetabolite on dipeptidase action. Had TblF made the Thr-TβL dipeptide isomer, the amino group of the TβL moiety would be tied up in an amide linkage and would not be available for the inactivating intramolecular lactam ring expansion. That would have increased the yield of active toxin eventually released by dipeptidase action in a plant cell. Instead in tabtoxin there is a built in clock for intramolecular destruction of the warhead both in tabtoxin dipeptide as well as tabtoxinine-β-lactam amino acid.

Acetyltransferase Activity of Ttr and Identification of Product (AcTβL). In addition to the two routes of self-protection noted in the sections above, (1) the intramolecular thermodynamically favored rearrangement of reactive acylating β-lactam to stable unreactive δ-lactam, and (2) the conversion of TβL to dipeptide, the producing *P. syringae* enable a third route of detoxification. This is the enzyme Ttr, where structural evidence and preliminary solution studies in a histone acetylation assay had indicated function as an acetyltransferase.[37−40] Despite cocrystallization with acetyl CoA nothing has been known about the selectivity of Ttr toward TβL versus the dipeptide tabtoxin or whether both the active TβL and the inactive TδL would be acetylation substrates. Further, the identity of the putative acetylated product was not known: one could envision acetyl transfer to the α-amino group, the β-lactam amide nitrogen, the OH group of the 5-hydroxy-β-lactam, and/or hydrolysis of the β-lactam ring during acetylation (Supporting Information, Figure S18).

We overproduced *P. syringae* Ttr in *E. coli* and purified it as a His-tagged enzyme in soluble form (yield = 22 mg/L; Supporting Information, Figure S3). Incubation of TβL (1 mM; generated from tabtoxin as noted earlier by dipeptidase action in *P. syringae* cell lysates) with one equivalent of acetyl-CoA and 25 μM Ttr led to quantitative conversion to a monoacetylated product, AcTβL, confirmed by HRMS. Interestingly, when the Ttr reaction mixture was quenched with Fmoc-Cl and analyzed by HPLC there was no detectable FmocTβL starting material, but also no visible new product peak. However, when the reaction mixture was analyzed by HPLC at 210 nm with no Fmoc-derivatization, a new more hydrophobic product peak was clearly present (Figure 5).

NMR analysis of the purified AcTβL product was also consistent with monoacetylation and showed that the β-lactam was still intact (Figure 6). One noticeable change in the ^{1}H NMR spectrum was that the α-hydrogen on C2 of AcTβL was shifted downfield by 0.4 ppm relative to the same signal for TβL. This was the first direct evidence that N1 might be the site of acetylation since the downfield shift of the C2 hydrogen could be rationalized through exposure to the deshielding cone of the acetyl group. Two-dimensional NMR spectroscopy (gCOSY, gHSQC, and gHMBC) confirmed that all the connectivities of the TβL backbone were still in place. Importantly, a key HMBC ^{1}H−^{13}C correlation was observed between the acetyl carbon, C8, and the hydrogen of the amino acid α carbon, C2, which provided strong evidence that N1 was the site of acetylation by Ttr (Figure 6a,b).

Separate studies indicated that Ttr does not acetylate the dipeptide tabtoxin, nor the δ-isomer either as the free amino acid, TδL, or dipeptide, TδL-Thr (data not shown). Since the α-amino group of the δ-isomers is tied up in an amide linkage it is reasonable that the δ-isomers are not substrates for Ttr acetylation. Since tabtoxin was not a substrate for Ttr, the presence of a C-terminal Thr residue must prevent recognition by the acetylase. L-Lysine and a number of analogs including N_6-formyl-L-lysine, N_6-acetyl-L-lysine, N_1-acetyl-L-lysine were also screened as Ttr substrates to gain further insight into the regioselectivity of Ttr acetylation. These substrates were incubated with Ttr (25 μM) in the presence of one equivalent

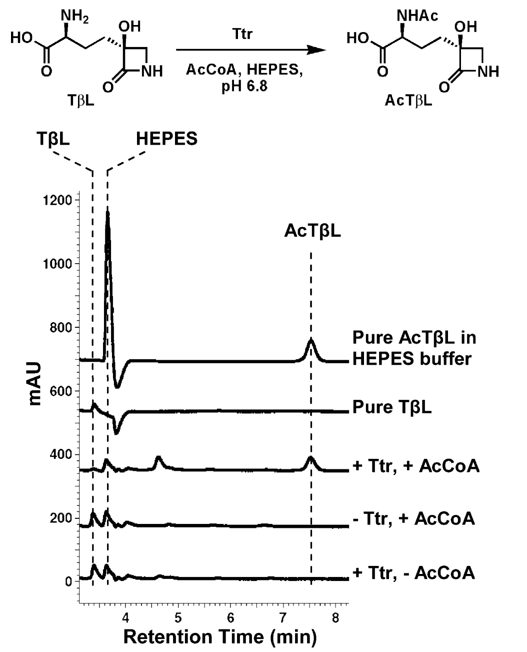

Figure 5. Characterization of Ttr activity by HPLC analysis with detection at 210 nm showing acetyl-CoA-dependent acetylation of TβL.

of acetyl-CoA and reaction mixtures were analyzed by high-resolution LC-MS after 24 h to search for acetylated products. None of the reactions went to completion, but reactions with L-lysine, N_6-formyl-L-lysine, and N_6-acetyl-L-lysine did produce an acetylated product consistent with acetylation of the free α-amino group. The reaction with N_1-acetyl-L-lysine gave no acetylated product which suggests that Ttr selectively acetylates α-amino groups as observed for the natural substrate tabtoxinine-β-lactam. (See the Supporting Information, Figures S19−S22 and Table S2, for high-res LC-MS data.)

The acetylation of TβL by Ttr plays a clear role in self-protection from the toxin since the acetylated product was proven to have no toxic effects on plants and bacteria.[36,38] However, a potential biosynthetic role for Ttr cannot yet be ruled out. Similar acetyltransferases have been reported to act early in the biosynthesis of other naturally occurring antimetabolites, such as the one encoded by the *bar* gene in bialaphos biosynthesis,[59] and it is the acetylated intermediates that are substrates for subsequent enzymatic transformations along the remaining biosynthetic pathway. Unlike the bialaphos acetyltransferase whose *bar* gene lies within the biosynthetic gene cluster, the acetyltransferase *ttr* gene is located outside of the tabtoxin biosynthetic gene cluster.[31,60]

AcTβL was not a substrate for the ligase even when excess L-Thr (20 mM) and large amounts of TblF enzyme (up to 10 μM) were used (data not shown). We tested AcTβL as a substrate for the recombinant TabP peptidase to see if this enzyme was acting as a deacetylase. No reaction was observed, but we still do not know if the recombinant TabP enzyme is active (data not shown). The fate of AcTβL (biosynthetic intermediate, recycled via deacetylase, or pro-drug?) is still unknown.

■ CONCLUSIONS

In this study we have isolated multimilligram quantities of tabtoxin dipeptide from a *P. syringae* producing strain (ATCC 11528), sufficient to characterize the rate of its rearrangement from the 5-hydroxy-β-lactam to the more stable off pathway 5-hydroxy-δ-lactam. In turn we have used the Zn^{2+}-dependent dipeptidase activity of *P. syringae* cell lysates to enable cleavage

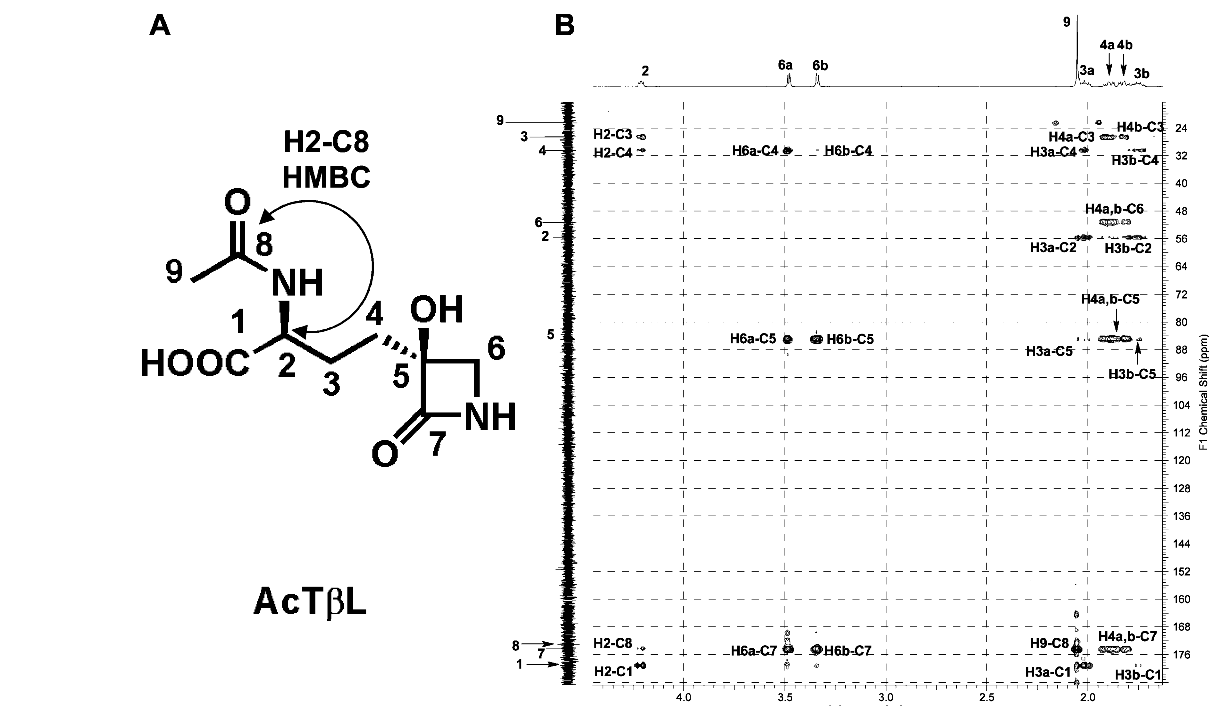

Figure 6. (A) Structure of AcTβL, N_1-acetyl-tabtoxinine-β-lactam, with the key $^1H-^{13}C$ HMBC correlation between H2 and C8 indicated by a double-headed arrow. (B) Gradient HMBCAC spectra of AcTβL at 600 MHz in D_2O containing 50 mM potassium phosphate at pH 5.4 with labeled $^1H-^{13}C$ correlations.

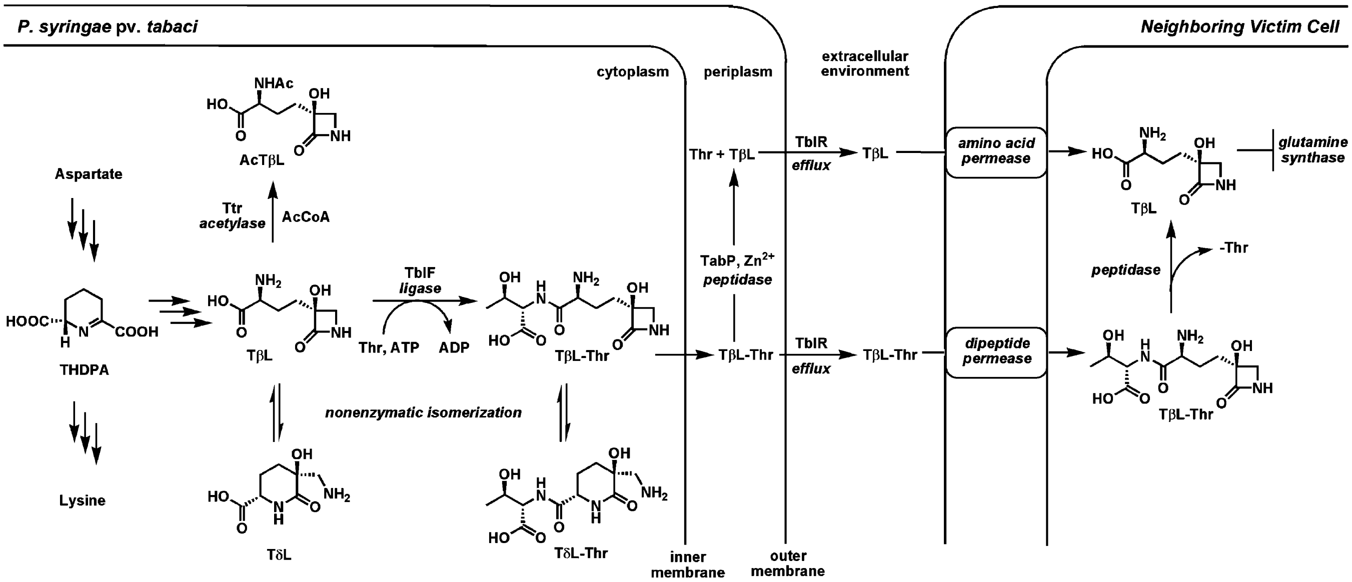

Figure 7. Biosynthesis of tabtoxinine-β-lactam (TβL) deviates from lysine biosynthesis at the level of tetrahydropicolinate (THDPA). Ligation of L-Thr and TβL by TblF in an ATP-dependent fashion generates the Trojan Horse dipeptide antibiotic tabtoxin (TβL-Thr) and provides a means of self-protection. Further self-protection is achieved by the action of acetylase Ttr which regioselectively acetylates the α-amino group of TβL. Both TβL and TβL-Thr degrade nonenzymatically to the biologically inactive δ-isomers, TδL and TδL-Thr, in a time and pH-dependent manner. Efflux of TβL-Thr, or TβL via the action of the periplasmic Zn-peptidase TabP, by TblR, a proposed membrane-bound member of the major facilitator superfamily of transporters,[64] to the extracellular environment exposes neighboring cells which can import the toxins via amino acid (TβL) or dipeptide (TβL-Thr) permeases.[20] Peptide bond cleavage of tabtoxin releases the tabtoxinine-β-lactam warhead,[18,19] which induces chlorosis via inhibition of glutamine synthase.[21]

of tabtoxin dipeptide under mild conditions to isolate the free amino acid component tabtoxinine-β-lactam (TβL) in multi-milligram quantities and also monitor its rate of intramolecular rearrangement to the biologically inactive δ-isomer (TδL). This rearrangement in both the free toxin amino acid and the Trojan Horse dipeptide constitutes an autoinactivating molecular clock built into the structure of the TβL scaffold and creates constraints on toxin isolation and assay development.

That molecular clock is one of three (or more[61−64]) ways (Figure 7) that the producer *P. syringae* cells protect themselves from unwanted suicidal action of TβL. The second is the TblF ligase-mediated conversion of TβL to dipeptide tabtoxin. This is a commonly used route for microbes to protect themselves from antimetabolite amino acids, as seen for example in alaphosphin,[65] microcin C7,[66,67] dapdiamide,[57] bacilysin,[54−56] phaseolotoxin,[68] and phosphinothricin pathways.[59,69] The di- to oligopeptide products now carry the antimetabolite chemical warhead in a latent form with respect to biological target recognition. Secretion by an export pump, represented by the *tblR* gene in the tabtoxin biosynthetic gene cluster, a fourth mechanism of self-protection in tabtoxin producers,[31,64] is followed at some later time by uptake by a susceptible neighboring cell (in this case plant cells on which the epiphytic *P. syringae* are growing[20]). Peptidase action within that victim cell releases the proximally toxic amino acid. The variant of Trojan Horse strategy in hiding TβL within the tabtoxin framework that is puzzling is why the TβL-Thr dipeptide rather than the Thr-TβL isomer is generated. In the latter the inactivating β- to δ-lactam ring expanding rearrangement would be blocked. As it is, some of the warhead is lost as that rearrangement proceeds in tabtoxin, lowering the chemical yield of the active toxin free amino acid subsequently delivered to plant cells, unless exposure of the toxin is maintained near a pH value of ~5, where both tabtoxin dipeptide and tabtoxinine-β-lactam amino acid are quite stable.

The third route of self-protection is the acetyltransferase Ttr, a member of the GNAT superfamily of acetyltransferases which are commonly evolved as resistance factors to antibiotics.[70] It is not clear at what point in the tabtoxinine-β-lactam/tabtoxin pathway this enzyme acts. It has been known that transfection of plants with this gene confers effective resistance to producer *P. syringae* infection.[36] The molecular basis of the inactivating modification catalyzed by Ttr also had been unknown. Here we have shown that Ttr regioselectively acetylates N1 of tabtoxinine-β-lactam using acetyl-CoA as a cosubstrate. The regioselective acetylation of α-amino groups was confirmed by showing that L-lysine, N_6-formyl-L-lysine, and N_6-acetyl-L-lysine were all substrates for Ttr while N_1-acetyl-L-lysine was not a substrate. Tabtoxin dipeptide, TβL-Thr, was not a substrate for Ttr presumably because the presence of a C-terminal amino acid residue prevents recognition by the enzyme. The δ-isomers, TδL-Thr and TδL, also were not substrates for Ttr presumably because the α-amino groups are tied up in amide linkages. Clearly, Ttr only recognizes and acetylates the active form of the toxic antimetabolite, TβL.

This initial study on characterization of the interconversion of TβL and tabtoxin by ligase acting synthetically and dipeptidase acting hydrolytically, in competition with intra-molecular rearrangement to the biologically dead δ-lactam forms, opens the way for subsequent study of molecular mechanism of the time-dependent inactivation of the TβL target glutamine synthetase. It also sets up investigation into the timing of the biosynthetic steps that build the unusual TβL 5-hydroxy-β-lactam warhead. There are three characterized distinct biosynthetic strategies to build β-lactams: in the penicillin and cephalosporins[71,72] by action of isoPenN synthase, in nocardicin monobactams where the β-lactam derives from a serine residue,[73−75] and in the clavams and carbapenems[76,77] via action of ATP-dependent β-lactam synthases on β-amino acid substrates.[41] There is a β-lactam synthase homologue as well as a nonheme iron oxygenase *orf* in the tabtoxin gene cluster (genes *tblS* and *tblC*, respectively[31]) so that route may also be in play for construction of the 5-hydroxy-β-lactam warhead of tabtoxinine-β-lactam.

■ ASSOCIATED CONTENT

Supporting Information

SDS-PAGE analysis of TabP, TblF, and Ttr purification. ^{1}H, ^{13}C, COSY, HSQC, and HMBC NMR spectra and HPLC traces of pure TβL-Thr, TδL-Thr, TβL, TδL, and AcTβL. Synthesis and NMR spectra of pure FormylLys-Thr, FormylLys-Ser, Fmoc-FormylLys-Thr, and Fmoc-FormylLys-Ser. First-order kinetic plots for rearrangement of TβL-Thr to TδL-Thr and TβL to TδL. HPLC traces and high-res LC-MS data for reactions of TblF ligase with a variety of amino acid substrates. Data plots for determination of TβL concentration and kinetic plots of dipeptide formation by the TblF-PK-LDH coupled assay. High-res LC-MS data for reactions of Ttr acetylase with a variety of amino acid substrates. This material is available free of charge via the Internet at http://pubs.acs.org.

■ AUTHOR INFORMATION

Corresponding Author

*E-mail: Christopher_Walsh@hms.harvard.edu. Phone: 617-432-1715. Fax: 617-432-0438.

Funding

This work was supported in part by National Institutes of Health Grants AI042738 and GM49338 (C.T.W.).

Notes

The authors declare no competing financial interest.

■ ACKNOWLEDGMENTS

We thank Dr. Jared B. Parker for assistance with cloning and protein purification as well as other helpful advice and discussions. We also thank Dr. Jared B. Parker for critical reading of this manuscript.

■ ABBREVIATIONS USED

E. coli, *Escherichia coli*; *P. syringae*, *Pseudomonas syringae*; TβL, tabtoxinine-β-lactam; TδL, tabtoxinine-δ-lactam; TβL-Thr, tabtoxin-L-threonine dipeptide; TβL-Ser, tabtoxin-L-serine dipeptide; TδL-Thr, isotabtoxin-L-threonine dipeptide; TδL-Ser, isotabtoxin-L-serine dipeptide; AcTβL, N_1-acetyl-tabtoxinine-β-lactam; FormylLys, N_6-formyl-L-lysine; Thr, L-threonine; Ser, L-serine; homoSer, L-homoserine; Ala, L-alanine; IPTG, isopropyl-β-D-galactopyranoside; SDS-PAGE, sodium dodecyl sulfate-polyacrylamide gel electrophoresis; HPLC, high performance liquid chromatography; HILIC, hydrophilic interaction chromatography; LC-MS, liquid chromatography−mass spectrometry; HRMS, high-resolution mass spectrometry; ESI, electrospray ionization; EIC, extracted ion chromatogram; NMR, nuclear magnetic resonance; FID, free induction decay; gCOSY, gradient homonuclear correlation spectroscopy; gHSQC, gradient heteronuclear single-quantum coherence; gHMBC, gradient heteronuclear multiple bond coherence; FPLC, fast protein liquid chromatography; PCR, polymerase chain reaction; NADH, reduced nicotinamide adenine dinucleotide; NAD^+, oxidized nicotinamide adenine dinucleotide; D_2O, deuterium oxide; HEPES, 2-[4-(2-hydroxyethyl)-piperazin-1-yl]ethanesulfonic acid; Tris, 2-amino-2-hydroxymethyl-propane-1,3-diol; TFA, trifluoroacetic acid; ATP, adenosine-5′-triphosphate; ADP, adenosine-5′-diphosphate; PEP, phosphoenolpyruvate; PK, pyruvate kinase; LDH, lactate dehydrogenase; Fmoc, fluorenylmethyloxycarbonyl; AcCoA, acetyl coenzyme A

■ REFERENCES

(1) Anzai, Y., Kim, H., Park, J.-Y., Wakabayashi, H., and Oyaizu, H. (2000) Phylogenetic affiliation of the pseudomonads based on 16S rRNA sequence. *Int. J. Syst. Evol. Microbiol.* 50, 1563−1589.

(2) Hwang, M. S. H., Morgan, R. L., Sarkar, S. F., Wang, P. W., and Guttman, D. S. (2005) Phylogenetic characterization of virulence and resistance phenotypes of *Pseudomonas syringae*. *Appl. Environ. Microbiol.* 71, 5182−5191.

(3) Kimura, M., Anzai, H., and Yamaguchi, I. (2001) Microbial toxins in plant-pathogen interactions: Biosynthesis, resistance mechanisms, and significance. *J. Gen. Appl. Microbiol.* 47, 149−160.

(4) Bender, C. L., Alarcón-Chaidez, F., and Gross, D. C. (1999) *Pseudomonas syringae* phytotoxins: Mode of action, regulation, and biosynthesis by peptide and polyketide synthetases. *Microbiol. Mol. Biol. Rev.* 63, 266−292.

(5) Arrebola, E., Cazorla, F. M., Pérez-García, A., and de Vicente, A. (2011) Genes involved in the production of antimetabolite toxins by *Pseudomonas syringae* pathovars. *Genes* 2, 640−660.

(6) Völksch, B., Bublitz, F., and Fritsche, W. (1989) Coronatine production by *Pseudomonas syringae* pathovars: Screening method and capacity of product formation. *J. Basic Microbiol.* 29, 463−468.

(7) Mittal, S., and Davis, K. R. (1995) Role of the phytotoxin coronatine in the infection of *Arabidopsis thaliana* by *Pseudomonas syringae* pv. *tomato*. *Mol. Plant-Microbe Interact.* 8, 165−171.

(8) Zheng, X.-Y., Weaver Spivey, N., Zheng, W., Liu, P.-P., Qing, Fu, Z., Klessig, D. F., Yang, He, S., and Dong, X. (2012) Coronatine promotes *Pseudomonas syringae* virulence in plants by activating a signaling cascade that inhibits salicylic acid accumulation. *Cell Host Microbe* 11, 587−596.

(9) Wäspi, U., Blanc, D., Winkler, T., Rüedi, P., and Dudler, R. (1998) Syringolin, a novel peptide elicitor from *Pseudomonas syringae* that induces resistance to *Pyricularia oryzae* in rice. *Mol. Plant-Microbe Interact.* 11, 727−733.

(10) Groll, M., Schellenberg, B., Bachmann, A. S., Archer, C. R., Huber, R., Powell, T. K., Lindow, S., Kaiser, M., and Dudler, R. (2008) A plant pathogen virulence factor inhibits the eukaryotic proteasome by a novel mechanism. *Nature* 452, 755−759.

(11) Mitchell, R. E. (1976) Isolation and structure of a chlorosis-inducing toxin of *Pseudomonas phaseolicola*. *Phytochemistry* 15, 1941−1947.

(12) Moore, R. E., and Niemczura, W. P. (1984) Inhibitors of ornithine carbamoyltransferase from *Pseudomonas syringae* pv. *phaseolicola*: Revised structure of phaseolotoxin. *Tetrahedron Lett.* 25, 3931−3934.

(13) Ballio, A., Barra, D., Bossa, F., Collina, A., Grgurina, I., Marino, G., Moneti, G., Paci, M., Pucci, P., Segre, A., and Simmaco, M. (1991) Syringopeptins, new phytotoxic lipodepsipeptides of *Pseudomonas syringae* pv. *syringae*. *FEBS Lett.* 291, 109−112.

(14) Hutchison, M. L., Tester, M. A., and Gross, D. C. (1995) Role of biosurfactant and ion channel-forming activities of syringomycin in transmembrane ion flux: A model for the mechanism of action in the plant-pathogen interaction. *Mol. Plant-Microbe Interact.* 8, 610−620.

(15) Woolley, D. W., Pringle, R. B., and Braun, A. C. (1952) Isolation of the phytopathogenic toxin of *Pseudomonas tabaci*, an antagonist of methionine. *J. Biol. Chem.* 197, 409−417.

(16) Stewart, W. W. (1971) Isolation and proof of structure of wildfire toxin. *Nature* 229, 174−178.

(17) Taylor, P. A., Schnoes, H. K., and Durbin, R. D. (1972) Characterization of chlorosis-inducing toxins from a plant pathogenic *Pseudomonas* sp. *Biochim. Biophys. Acta* 286, 107−117.

(18) Durbin, R. D., and Uchytil, T. F. (1984) The role of intercellular fluid and bacterial isolate on the *in vivo* production of tabtoxin and tabtoxinine-β-lactam. *Physiol. Plant Pathol. 24*, 25−31.

(19) Levi, C., and Durbin, R. D. (1986) The isolation and properties of a tabtoxin-hydrolysing aminopeptidase from the periplasm of *Pseudomonas syringae* pv. *tabaci*. *Physiol. Mol. Plant Pathol. 28*, 345−352.

(20) Bush, D. R., and Langston-Unkefer, P. J. (1987) Tabtoxinine-β-lactam transport into cultured corn cells: Uptake via an amino acid transport system. *Plant Physiol. 85*, 845−849.

(21) Sinden, S. L., and Durbin, R. D. (1968) Glutamine synthetase inhibition: Possible mode of action of wildfire toxin from *Pseudomonas tabaci*. *Nature 219*, 379−380.

(22) Thomas, M. D., Langston-Unkefer, P. J., Uchytil, T. F., and Durbin, R. D. (1983) Inhibition of glutamine synthetase from pea by tabtoxinine-β-lactam. *Plant Physiol. 71*, 912−915.

(23) Langston-Unkefer, P. J., Macy, P. A., and Durbin, R. D. (1984) Inactivation of glutamine synthetase by tabtoxinine-β-lactam. *Plant Physiol. 76*, 71−74.

(24) Thomas, M. D., and Durbin, R. D. (1985) Glutamine synthetase from *Pseudomonas syringae* pv. *tabaci*: Properties and inhibition by tabtoxinine-β-lactam. *J. Gen. Microbiol. 131*, 1061−1067.

(25) Wolf, F. A., and Foster, A. C. (1917) Bacterial leaf spot of tobacco. *Science 46*, 361−362.

(26) Unkefer, C. J., London, R. E., Durbin, R. D., Uchytil, T. F., and Langston-Unkefer, P. J. (1987) The biosynthesis of tabtoxinine-β-lactam. *J. Biol. Chem. 262*, 4994−4999.

(27) Müller, B., Hädener, A., and Tamm, C. (1987) 48. Studies on the biosynthesis of tabtoxin (wildfire toxin). Origin of the carbonyl C-atom of the β-lactam moiety from the C_1-pool. *Helv. Chim. Acta 70*, 412−422.

(28) Roth, P., Hädener, A., and Tamm, C. (1990) 52. Further studies on the biosynthesis of tabtoxin (wildfire toxin): Incorporation of $[2,3\text{-}^{13}C_2]$pyruvate into the β-lactam moiety. *Helv. Chim. Acta 73*, 476−482.

(29) Kinscherf, T. G., Coleman, R. H., Barta, T. M., and Willis, D. K. (1991) Cloning and expression of the tabtoxin biosynthetic region from *Pseudomonas syringae*. *J. Bacteriol. 173*, 4124−4132.

(30) Barta, T. M., Kinscherf, T. G., Uchytil, T. F., and Willis, D. K. (1993) DNA Sequence and transcriptional analysis of the *tblA* gene required for tabtoxin biosynthesis by *Pseudomonas syringae*. *Appl. Environ. Microbiol. 59*, 458−466.

(31) Kinscherf, T. G., and Willis, D. K. (2005) The biosynthetic gene cluster for the β-lactam antibiotic tabtoxin in *Pseudomonas syringae*. *J. Antibiot. 58*, 817−821.

(32) Engst, K., and Shaw, P. D. (1992) Identification of a *lysA*-like gene required for tabtoxin biosynthesis and pathogenicity in *Pseudomonas syringae* pv. *tabaci* strain PTBR2.024. *Mol. Plant-Microbe Interact. 5*, 322−329.

(33) Liu, L., and Shaw, P. D. (1997) Characterization of *dapB*, a gene required by *Pseudomonas syringae* pv. tabaci BR2.024 for lysine and tabtoxinine-β-lactam biosynthesis. *J. Bacteriol. 179*, 507−513.

(34) Liu, L., and Shaw, P. D. (1997) A possible role for acetylated intermediates in diaminopimelate and tabtoxinine-β-lactam biosynthesis in *Pseudomonas syringae* pv. tabaci BR2.024. *J. Bacteriol. 179*, 5922−5927.

(35) Anzai, H., Yoneyama, K., and Yamaguchi, I. (1990) The nucleotide sequence of tabtoxin resistance gene (*ttr*) of *Pseudomonas syringae* pv. *tabaci*. *Nucleic Acids Res. 18*, 1890.

(36) Anzai, H., Yoneyama, K., and Yamaguchi, I. (1989) Transgenic tobacco resistant to a bacterial disease by the detoxification of a pathogenic toxin. *Mol. Gen. Genet. 219*, 492−494.

(37) Neuwald, A. F., and Landsman, D. (1997) GCN5-related histone *N*-acetyltransferases belong to a diverse superfamily that includes the yeast SPT10 protein. *Trends Biol. Sci. 22*, 154−155.

(38) Liu, J., Le, Y., Zhen, Y., Zhu, C., Shen, J., and Zhang, R. (2002) Tabtoxin-resistant protein: Overexpression, purification, and characterization. *Protein Expression Purif. 24*, 439−444.

(39) Ding, Y., Li, S., Li, X., Sun, F., Liu, J., Zhao, N., and Rao, Z. (2003) Site-directed mutagenesis and preliminary X-ray crystallographic studies of the tabtoxin resistance protein. *Protein Pept. Lett 10*, 255−263.

(40) He, H., Ding, Y., Bartlam, M., Sun, F., Le, Y., Qin, X., Tang, H., Zhang, R., Joachimiak, A., Liu, J., Zhao, N., and Rao, Z. (2003) Crystal structure of tabtoxin resistance protein complexed with acetyl coenzyme A reveals the mechanism for β-lactam acetylation. *J. Mol. Biol. 325*, 1019−1030.

(41) Bachmann, B. O., Li, R., and Townsend, C. A. (1998) β-Lactam synthetase: A new biosynthetic enzyme. *Proc. Natl. Acad. Sci. U. S. A. 95*, 9082−9086.

(42) Janc, J. W., Egan, L. A., and Townsend, C. A. (1995) Purification and characterization of clavaminate synthase from *Streptomyces antibioticus*. *J. Biol. Chem. 270*, 5399−5404.

(43) Kiyota, H., Takai, T., Shimasaki, Y., Saitoh, M., Nakayama, O., Takada, T., and Kuwahara, S. (2007) Synthesis of (-)-tabtoxinine-β-lactam, the phytotoxin of tobacco wildfire disease. *Synthesis*, 2471−2480.

(44) Lee, D. L., and Rapoport, H. (1975) Synthesis of tabtoxinine-δ-lactam. *J. Org. Chem. 40*, 3491−3495.

(45) Baldwin, J. E., Bailey, P. D., Gallacher, G., Singleton, K. A., and Wallace, P. M. (1983) Stereospecific synthesis of tabtoxin. *J. Chem. Soc., Chem. Commun.*, 1049−1050.

(46) Baldwin, J. E., Bailey, P. D., and Gallacher, G. (1984) Stereospecific synthesis of tabtoxin. *Tetrahedron 40*, 3695−3708.

(47) Baldwin, J. E., Otsuka, M., and Wallace, P. M. (1986) Synthetic studies on tabtoxin. Synthesis of a naturally occuring inhibitor of glutamine synthetase, tabtoxinine-β-lactam, and analogues. *Tetrahedron 42*, 3097−3110.

(48) Baldwin, J. E., Fieldhouse, R., and Russell, A. T. (1993) Synthesis and assignment of the relative stereochemistry of a putative biosynthetic precursor of tabtoxinine β-lactam. *Tetrahedron Lett. 34*, 5491−5494.

(49) Kiyota, H., Takai, T., Saitoh, M., Nakayama, O., Oritani, T., and Kuwahara, S. (2004) Facile synthesis of (-)-tabtoxinine-β-lactam and its (3′*R*)-isomer. *Tetrahedron Lett. 45*, 8191−8194.

(50) Welch, M., Govindarajan, S., Ness, J. E., Villalobos, A., Gurney, A., Minshull, J., and Gustafsson, C. (2009) Design parameters to control synthetic gene expression in *Escherichia coli*. *PLoS ONE 4*, e7002.

(51) Heemstra, J. R., Walsh, C. T., and Sattely, E. S. (2009) Enzymatic tailoring of ornithine in the biosynthesis of the *Rhizobium* cyclic trihydroxamate siderophore vicibactin. *J. Am. Chem. Soc. 131*, 15317−15329.

(52) Horecker, B., and Kornberg, A. (1948) The extinction coefficients of the reduced band of pyridine nucleotides. *J. Biol. Chem. 175*, 385−390.

(53) Galperin, M. Y., and Koonin, E. V. (1997) A diverse superfamily of enzymes with ATP-dependent carboxylate-amine/thiol ligase activity. *Protein Sci. 6*, 2639−2643.

(54) Tabata, K., Ikeda, H., and Hashimoto, S.-I. (2005) *ywfE* in *Bacillus subtilis* codes for a novel enzyme, L-amino acid ligase. *J. Bacteriol. 187*, 5195−5202.

(55) Tabata, K., and Hashimoto, S.-I. (2007) Fermentative production of L-alanyl-L-glutamine by a metabolically engineered *Escherichia coli* strain expressing L-amino acid α-ligase. *Appl. Environ. Microbiol. 73*, 6378−6385.

(56) Shomura, Y., Hinokuchi, E., Ikeda, H., Senoo, A., Takahashi, Y., Saito, J.-I., Komori, H., Shibata, N., Yonetani, Y., and Higuchi, Y. (2012) Structural and enzymatic characterization of BacD, an L-amino acid dipeptide ligase from *Bacillus substilis*. *Protein Sci. 21*, 707−716.

(57) Hollenhorst, M. A., Clardy, J., and Walsh, C. T. (2009) The ATP-dependent amide ligases DdaG and DdaF assemble the fumaramoyl-dipeptide scaffold of the dapdiamide antibiotics. *Biochemistry 48*, 10467−10472.

(58) Harzallah, D., and Laous, L. (1998) The synthesis of tabtoxin peptide bond in *Pseudomonas syringae* pv. *tabaci*. *Biochem. Soc. Trans. 26*, S383.

(59) Kumada, Y., Anzai, H., Takano, E., Murakami, T., Hara, O., Itoh, R., Imai, S., and Satoh, A. (1988) The bialaphos resistance gene (*bar*) plays a role in both self-defense and bialaphos biosynthesis in *Streptomyces hygroscopicus*. *J. Antibiot. 41*, 1838−1845.

(60) Studholme, D. J., Gimenez Ibanez, S., MacLean, D., Dangl, J. L., Chang, J. H., and Rathjen, J. P. (2009) A draft genome sequence and functional screen reveals the repertoire of type III secreted proteins of *Pseudomonas syringae* pathovar *tabaci* 11528. *BMC Genomics 10*, 394−413.

(61) Knight, T. J., Durbin, R. D., and Langston-Unkefer, P. J. (1986) Role of glutamine synthetase adenylation in the self-protection of *Pseudomonas syringae* subsp. "*tabaci*" from its toxin, tabtoxinine-β-lactam. *J. Bacteriol. 166*, 224−229.

(62) Knight, T. J., Durbin, R. D., and Langston-Unkefer, P. J. (1987) Self-protection of *Pseudomonas syringae* pv. "*tabaci*" from its toxin, tabtoxinine-β-lactam. *J. Bacteriol. 169*, 1954−1959.

(63) Coleman, R. H., Shaffer, J., and True, H. (1996) Properties of β-lactamase from *Pseudomonas syringae*. *Curr. Microbiol. 32*, 147−150.

(64) Saier, J., M. H., Beatty, J. T., Goffeau, A., Harley, K. T., Heijne, W. H. M., Huang, S.-C., Jack, D. L., Jähn, P. S., Lew, K., Liu, J., Pao, S. S., Paulsen, I. T., Tseng, T.-T., and Virk, P. S. (1999) The major facilitator superfamily. *J. Mol. Microbiol. Biotechnol. 1*, 257−279.

(65) Atherton, F. R., Hall, M. J., Hassall, C. H., Lambert, R. W., Lloyd, W. J., and Ringrose, P. S. (1979) Phosphonopeptides as antibacterial agents: Mechanism of action of alaphosphin. *Antimicrob. Agents Chemother. 15*, 696−705.

(66) Agarwal, V., Metlitskaya, A., Severinov, K., and Nair, S. K. (2011) Structural basis for microcin C7 inactivation by the MccE acetyltransferase. *J. Biol. Chem. 286*, 21295−21303.

(67) Agarwal, V., Tikhonov, A., Metlitskaya, A., Severinov, K., and Nair, S. K. (2012) Structure and function of a serine carboxypeptidase adapted for degradation of the protein synthesis antibiotic microcin C7. *Proc. Natl. Acad. Sci. U. S. A. 109*, 4425−4430.

(68) Arai, T., and Kino, K. (2008) A novel L-amino acid ligase is encoded by a gene in the phaseolotoxin biosynthetic gene cluster from *Pseudomonas syringae* pv. *phaseolicola* 1448A. *Biosci. Biotechnol. Biochem. 72*, 3048−3050.

(69) Blodgett, J. A. V., Zhang, J. K., and Metcalf, W. W. (2005) Molecular cloning, sequence analysis, and heterologous expression of the phosphinothricin tripeptide biosynthetic gene cluster from *Streptomyces viridochromogenes* DSM 40736. *Antimicrob. Agents Chemother. 49*, 230−240.

(70) Vetting, M. W., de Carvalho, L. P. S., Yu, M., Hegde, S. S., Magnet, S., Roderick, S. L., and Blanchard, J. S. (2005) Structure and function of the GNAT superfamily of acetyltransferases. *Arch. Biochem. Biophys. 433*, 212−226.

(71) Roach, P. L., Clifton, I. J., Hensgens, C. M. H., Shibata, N., Schofield, C. J., Hajdu, J., and Baldwin, J. E. (1997) Structure of isopenicillin *N* synthase complexed with substrate and the mechanism of penicillin formation. *Nature 387*, 827−830.

(72) Clifton, I. J., Ge, W., Adlington, R. M., Baldwin, J. E., and Rutledge, P. J. (2011) The crystal structure of isopenicillin N synthase with δ-(L-α-aminoadipoyl)-L-cysteinyl-D-methionine reveals thioether coordination to iron. *Arch. Biochem. Biophys. 516*, 103−107.

(73) Townsend, C. A., and Brown, A. M. (1983) Nocardicin A: Biosynthetic experiments with amino acid precursors. *J. Am. Chem. Soc. 105*, 913−918.

(74) Townsend, C. A., Brown, A. M., and Nguyen, L. T. (1983) Nocardicin A: Stereochemical and biomimetic studies of monocyclic β-lactam formation. *J. Am. Chem. Soc. 105*, 919−927.

(75) Gunsior, M., Breazeale, S. D., Lind, A. J., Ravel, J., Janc, J. W., and Townsend, C. A. (2004) The biosynthetic gene cluster for a monocyclic β-lactam antibiotic, nocardicin A. *Chem. Biol. 11*, 927−938.

(76) Miller, M. T., Bachmann, B. O., Townsend, C. A., and Rosenzweig, A. C. (2001) Structure of β-lactam synthetase reveals how to synthesize antibiotics instead of asparagine. *Nat. Struct. Biol. 8*, 684−689.

(77) Miller, M. T., Gerratana, B., Stapon, A., Townsend, C. A., and Rosenzweig, A. C. (2003) Crystal structure of carbapenam synthetase (CarA). *J. Biol. Chem. 278*, 40996−41002.